PRE-HEATING OF WOOD CHIPS BY SIMULATED KRAFT RECOVERY BOILER FLUE GASES

Final Report

by

A.P. Watkinson and B. Chow
Department of Chemical Engineering
The University of British Columbia
Vancouver, B.C. V6T 1W5

Work on this project was conducted under the auspices of the Canada Centre for Mineral and Energy Technology - Energy, Mines and Resources Canada.

DSS File No. 20SU-2-9086
DSS Contract Serial No. ISU82-00232
CANMET Project No.
CANMET Scientific Authority: R. Braaten

Date: March 1985

This report should be cited as Contract Report No. ISU82-00232.

JUL 03 1985

MICROMEDIA

58 pp

SUMMARY

Heat transfer rates from gases to wood-chips were measured by an unsteady state technique. Hot air and air/steam mixtures at about 130°C were passed upwards through 0.2-m dia. x 1-m deep packed beds of Douglas-fir wood chips which had previously been screened for size. Temperatures were measured in the gas phase as a function of time and position, and heat transfer coefficients from the gas to the solids determined using a mathematical model. The model was developed assuming plug flow of gas through a packed bed of slab-shaped particles with finite internal thermal resistance. The effects of gas velocity, wood chip thickness, and presence of steam on the heat transfer coefficients were determined. In some experiments internal wood-chip temperatures were also measured. Pressure drop data were taken over a range of air velocities at room temperature. Heat transfer and pressure drop data are compared with information on irregularly shaped particles in the literature, and some recommendations made for use in design of chip pre-heating equipment.

TABLE OF CONTENTS

		Page
	Summary	
1.	Nomenclature	i
2.	Introduction	1
3.	Analysis of Heat Transfer in Adiabatic Packed Beds	4
4.	Experimental Work	9
5.	Procedure and Calculation of Heat Transfer Coefficient	10
6.	Heat Transfer Results 1. Verification Tests on Spherical Particles 2. Dry Air to Dry Wood Chip Heat Transfer 3. Moist Air to Dry Wood Chip Heat Transfer 4. Correlation and Comparison with Literature	11
7.	Pressure Drop Results	16
8.	Conclusions	17
9.	Further work	18
10.	References	19
Appendix	A. Work Statement	

ACKNOWLEDGEMENT

The authors wish to acknowledge the useful advice and suggestions of Dr. B. Blackwell during the formulation and experimental phases of this work.

LIST OF FIGURES

Figure No.		Page
1.	Literature correlation of heat transfer results	23
2.	Transient heating curves for slab-shaped single particles	24
3.	Theoretical temperature profiles for a bed of spheres	25
4.	Theoretical temperature profiles for a bed of slabs	26
5.	a) Schematic of apparatus b) Detail of column	27,28
6.	Photographs of particles	29,30
7.	Typical result of temperature measurements versus time for spherical particles	31
8.	Temperature profiles for spheres at a) Re_p = 87 b) Re_p = 169 and c) Re_p = 228	32
9.	Comparison of Spherical Particle Data with Literature Values	33
10.	Temperature profiles for 2.44-mm wood chips at a) Re_p = 255 b) Re_p = 329 c) Re_p = 403 d) Re_p = 476	34,35
11.	Temperature profiles for 4.03-mm wood chips at a) Re_p = 374 b) Re = 482 c) Re_p = 590 d) Re_p = 693	36,37
12.	Temperature profiles for 7.26-mm wood chips at a) Re_p = 491 b) Re_p = 633 c) Re_p = 774	38
13.	Temperature profiles for mixed wood chips 4.8-mm thick a) Re_p = 399 b) Re_p = 630	39
14.	Internal wood chip and gas temperature for a) 2.44-mm thick chips and b) 4.03-mm thick chips	40
15.	Comparison of temperature profiles for dry and moist air a) 4.03-mm thick chips and b) 7.26-mm thick chips	41
16.	Correlation of heat transfer coefficient vs. Reynolds number and superficial velocity	42,43
17.	Comparison of wood-chip data with literature values	44
18.	Plot of h_T versus Velocity	45
19.	Pressure drop data for spherical particles	46

LIST OF FIGURES
(continued)

Figure No.		Page
20.	Experimental pressure drop versus Ergun equation prediction for wood chips of thickness a) 2.44-mm b) 4.03-mm c) 7.26-mm d) 4.8 mm (mixed)	47,48
21.	Experimental pressure drop versus Ergun equation predictions with fitted voidage and sphericity.	49,50
22.	Pressure drop versus velocity for wood chips.	51

LIST OF TABLES

1.	Properties of Wood Chips and Spherical Particles	20
2.	Heat Transfer Test Conditions and Results for Spherical Particles	21
3.	Heat Transfer Test Conditions and Results for Wood Chips	22

NOMENCLATURE

a, a_{nom}, a_T	Surface area per unit volume of bed (eq'ns 25,26)
Cp_f, Cp_s	Heat capacity of fluid (air) and solid
h_f, h_T	Heat transfer film coefficients from gas to solid based on $a_{nominal}$ and a_T respectively.
k, k_s	Thermal conductivity of gas, of solid
L	One half the chip thickness
P	Pressure
Q	Heat flow
r, r_x	Radial component, distance component
R	Radius of sphere
T, T_o	Gas (air) temperature, gas temperature at bed inlet
t, t_i	Solid temperature, solid temperature at time zero.
V	Superficial velocity
W	Width of wood chip
Y	Dimension less group (eq'n 6)
Z	Dimension less group (eq'n 6)
z	Distance along packed bed

α	Thermal diffusivity	Bi	Biot number
ε	Voidage of packed bed	Re	Reynolds number
θ	Time	Fo	Fourier number
ρ_g, ρ_s	Density of gas, solid	Nu	Nusselt number

2. Introduction

The preheating of wood chips by flue gases prior to pulping in order to save on steam requirements in the digester has been proposed by Blackwell et al. (1,2). In their proposed process the design of the chip pre-heating vessel was based on generalized pressure drop and heat transfer equations for packed beds of regular solids, since no data were available for heat transfer and pressure drop specifically for wood chips. This lack of sound data necessitated a particularly conservative design because of the inherent uncertainties in dealing with transfer processes to particles as irregular in shape as typical wood chips.

The aims of this work were to obtain such data in packed beds of wood chips so that a sound design method could be used. The specific details to be studied are found in the attached work statement (Appendix A). The general approach taken was to carry out un-steady state heat transfer experiments in which a fixed bed of wood chips is heated by air at about 120-150°C, either dry or containing quantities of moisture up to 30% wt. The unsteady state approach simplifies the equipment in that chip feed and recovery systems are eliminated, although the measurement and interpretation of time-dependent phenomena are more difficult. For example in heating an initially cold bed of wood chips with hot gas, a temperature wave will pass through the bed, and temperatures will change as a function of both bed height and time. If a moist gas is used, condensation of steam on the bed of particles will occur along with convection in the colder part of the bed causing an increase in the rate of bed heat-up. Eventually the water will be driven off, and convection to the surface will remain as the dominant heat transfer mechanism. The transfer process will thus be different during the condensation and evaporation periods, and also will differ from results where no phase change occurs.

If one considers the heat transfer mechanisms at work in this process, then one must be concerned with

(i) condensation of steam onto beds of wood chips

(ii) convection from hot gases to surface of wood chip

(iii) conduction within the solid wood chip

(iv) evaporation of condensed water from the surace of the wood chip, which involves a mass transfer of vapour into the surrounding gas.

Given the current state of knowledge of the heat and mass transfer processes occurring, it appeared that the key part of the initial studies should involve sensible heat transfer to the wood chip bed with the associated internal conduction problem. The condensation was next in importance, as it will speed up the heating process. Knowing the heat transfer coefficient to the dry wood chip surface, the mass transfer coefficient describing the transfer of vapour from the chip surface can, in principle, be calculated.

There is a considerable body of experimental work on heat transfer coefficients between gases and beds of fine, regular solids. One such collection of data (3) from many investigators is shown in Fig. 1. Two features are noteworthy. A relatively good fit of data is available up to $Re_p = 10$ for data on fine solids of $d_p < 1$ mm, however for higher Reynolds numbers the extent of scatter is significant. Considering the parameters of the design of Blackwell et al. (1,2), where the flue gas velocity ~ 1.1 m/s, and given the real size of wood chips say 25.4 mm wide x 6 mm thick x 50 mm long (Vol. = 7620 mm^3), the particle Reynolds number can be estimated. The equivalent diameter is $d_e = 2\left(\frac{Vol}{4\pi/3}\right)^{1/3} = 24$ mm, whence the particle Reynolds number is $Re_p = V\, de/\nu = (1.1)(24\times10^{-3})/(25\times10^{-6}) = 1060$.

Clearly for wood chips in a real vessel, the Reynolds number is such that given the data of Fig. 1, the Nusselt number is rather uncertain but it should be Nu ~ 50, whence h_f = 65 W/m^2K. This is the external film coefficient and does not include the resistance to internal conduction.

Because wood is a relatively low conductivity material, and the wood chip is relatively thick, there will be a considerable internal thermal resistance. For a slab-like geometry 2L in thickness, the internal resistance will be $R_s = L/k_s$ and given typical values of chip thickness of 6 mm and reported thermal conductivity of k_s = 0.17 W/mK, then R_s = $3*10^{-3}/0.17$ = .018 $(W/mK)^{-1}$. Thus the Biot number $Bi = h_f L/k_s$ = 1.0. The overall coefficient from the gas to the solid interior is $U = (\frac{1}{h_f} + R_s)^{-1}$ = 30 W/m^2K. These very rough calculations show that the internal thermal resistance is about equal to the outside gas film resistance and thus both factors would have to be considered. One should also note that although condensation coefficients for pure steam onto solids are very high, this effect will be reduced in a 30% H_2O stream. In the event that moisture-laden gases are used to heat the solids the maximum expected overall coefficient, U, will be about ~ 40 W/m^2K.

The time for the internal conduction process to occur can be analyzed for single particles using graphical solutions to the heat conduction problem (4). Thus, Fig. 2 shows how the temperature profiles within a single particle should change as a function of time for various values of the Biot number, which gives the relative importance of the internal conduction resistance to the convection resistance. Given the above properties for the wood chip as described, the heat-up period to bring the particle centre-line temperature to about 80°C should be about 60 s. when surrounded by air at 150°C. In a real process as the air passes through the bed the temperature

and the time to reach 80°C will be considerably longer.

The single-particle method is not easily incorporated into the fixed-bed situation, except by trial and error, since the gas temperature is a function of distance and time. The approach taken was to write a mathematical description of the packed bed which includes the gas and solids heat balances.

Analysis of Heat Transfer in Adiabatic Packed Beds

For dry particles, heat transfer to a packed bed of particles will be modeled for several cases. The basic situation is shown in the sketch below:

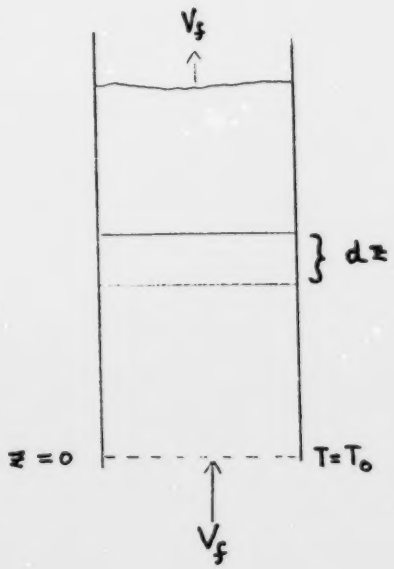

In all the models taken below, the following assumptions are made:

(i) The gas is in plug flow (-i.e. no radial or axial mixing) and at a constant velocity.

(ii) conduction in the axial direction can be neglected.

(iii) properties of the gas and the solids are independent of temperature.

(iv) at time zero the bed is at a uniform temperature t_i. The gas then enters at a temperature T_o.

(v) there is no heat loss or gained through the walls of the column (adiabatic).

Case 1. Negligible thermal resistance inside particles

This situation applies to small or high conductivity particles where the temperature inside the particles is uniform. It is mentioned here because it is used to verify the model used subsequently. The equations are as follows:

Enthalpy balance on gas:

$$-V_f C_{p_f} \rho_f \frac{\partial T}{\partial z} - h a (T-t) = \epsilon C_{p_f} \rho_f \frac{\partial T}{\partial \theta} \qquad (1)$$

Balance on solid

$$h a (T-t) = (1-\epsilon) C_{p_s} \rho_s \frac{\partial t}{\partial \theta} \qquad (2)$$

Initial and boundary conditions

$$\left.\begin{aligned} T = T_o \;,\; t = t_i \;\text{ all } z \;,\; \theta = 0 \\ T = T_o \;,\; z = 0 \;,\; \text{all } \theta \end{aligned}\right\} \qquad (3)$$

The solution was given by Anzelius (5)

$$t = T_o \int_0^{\infty} I_o (2\sqrt{YZ})\, e^{-Y} e^{-Z}\, dZ \qquad (4)$$

$$T = t + T_o\, I_o (2\sqrt{YZ})\, e^{-Y} e^{-Z} \qquad (5)$$

where $$Y = \frac{h a z}{\rho_f C_{p_f} V_f} \;, \quad Z = \frac{h a \theta}{\rho_f C_{p_f} (1-\epsilon)} \qquad (6)$$

and I_o is a Bessel function.

Case 2: Spherical particles with finite internal thermal resistance

This case applies to the low-conductivity spheres used to check the validity of the equipment and techniques. The basic equations are

Enthalpy balance on gas

$$-V_f C_{p_f} \rho_f \frac{\partial T}{\partial z} - ha\,(T - t_{r=R}) = \epsilon C_{p_f} \rho_f \frac{\partial T}{\partial \theta} \qquad (7)$$

Conduction inside sphere

$$k_s \left(\frac{\partial^2 t}{\partial r^2} + \frac{2}{r} \frac{\partial t}{\partial r} \right) = C_{p_s} \rho_s \frac{\partial t}{\partial \theta} \qquad (8)$$

At surphace of sphere

$$h\,(T - t_{r=R}) = -k_s \frac{\partial t}{\partial r}\Big)_{r=R} \qquad (9)$$

At the centre of the sphere, symmetry holds

$$\frac{\partial t}{\partial r} = 0 \qquad \text{all } z, \theta \qquad (10)$$

These equations were solved by Rosen (6) for an ion-exchange problem. In heat transfer terms, a solution obtained by the method of Amundson (7,8) but using Rosen's (6) function is

$$T(z,\theta) = (T_0 - t_i)\,\Phi + t_i \qquad (11)$$

$$t_{r=R} = T + (T_0 - t_i) \frac{\partial \Phi}{\partial \bar{X}} \cdot \frac{1}{Bi} \qquad (12)$$

where

$$\Phi = \frac{1}{2} + \frac{1}{\pi} \int_0^\infty e^{-\bar{X} H_1} \sin\left[\frac{2\eta\beta}{\alpha} - \bar{X} H_2 \right] \frac{d\beta}{\beta} \qquad (13)$$

where

$$\bar{X} = 3(1-\epsilon) \frac{z}{V_f} \frac{k_s}{R^2 C_{p_f} \rho_f} \qquad (14)$$

$$\eta/\alpha = \left(Fo - \frac{z}{V_f}\frac{\alpha_s \epsilon}{R^2}\right)$$

$$H_1 = \frac{HD_1 + \frac{1}{Bi}\left(HD_1^2 + HD_2^2\right)}{(1 + HD_1/Bi)^2 + (HD_2/Bi)^2} \qquad H_1\ (\lim \beta \to 0) = 0$$

$$H_2 = \frac{HD_2}{(1 + HD_1/Bi)^2 + (HD_2/Bi)^2} \qquad H_2\ (\lim \beta \to 0) = 0$$

$$HD_1 = \frac{\lambda(\sinh 2\lambda + \sin 2\lambda)}{\cosh 2\lambda - \cos 2\lambda} - 1 \qquad HD_1\ (\lim \beta > 64) = \sqrt{\beta} - 1$$
$$(\lim \beta < .1) = \frac{4\beta^2}{45}$$

$$HD_2 = \frac{\lambda(\sinh 2\lambda - \sin 2\lambda)}{\cosh 2\lambda - \cos 2\lambda} \qquad HD_2\ (\lim \beta > 64) = \sqrt{\beta}$$
$$(\lim \beta < .1) = \frac{2}{3}\beta$$

$$\lambda = \sqrt{\beta} \qquad (15)$$

$$\lim \beta \to 0 \quad \sin\left[\frac{2\eta\beta}{\alpha} - \bar{\gamma} H_2\right] = \frac{2\eta}{\alpha} - \frac{2}{3}\bar{x}$$

Thus the solution is a function of three dimensionless groups, the Biot number, a Fourier number (η/σ), and a dimensionless length $\bar{x}$. Figure 3 is a plot of this solution for spheres of low conductivity. As Bi → 0 the solution approaches that of Anzelius.

Case 3: Slab-shaped particles with finite internal resistance

Since no solution of the problem of heat transfer to a packed bed of slab-shaped particles was available in the literature, a solution was developed by B. Chow (9) for this work. The equations are

Enthalpy balance on gas

$$-V_f C_{p_f} \rho_f \frac{\partial T}{\partial z} - h a (T - t_{r=L}) = \epsilon C_{p_g} \rho_g \frac{\partial T}{\partial \theta} \qquad (16)$$

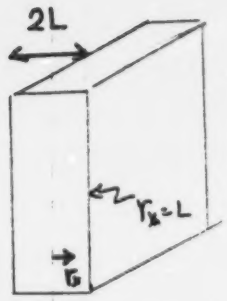

conduction within the chip

$$k_s \frac{\partial^2 t}{\partial r_x^2} = C_{ps} \rho_s \frac{\partial t}{\partial \theta} \qquad (17)$$

Particle surface

$$h(T - t_{r_x=L}) = -k_s \frac{\partial t}{\partial r_x}\Big|_{r_x=L} \qquad (18)$$

Symmetry was assumed at $r_x = 0$ i.e.

$$\frac{\partial t}{\partial r_x} = 0 \quad \text{at} \quad r_x = 0 \qquad (19)$$

The solution of this set of equations is used to generate the heat transfer coefficient values from experimental gas temperature profiles measured as a function of position and time. The mathematical solution to this problem is very complicated, and is given in detail in the M.A.Sc. thesis of B. Chow (9). The final equations are presented below:

$$T(z,\theta) = (T_0 - t_i)\,\Phi + t_i \qquad (20)$$

$$t_{r_x=L} = T + (T_0 - t_i)\frac{\partial \Phi}{\partial \bar{X}} \cdot \frac{1}{Bi} \qquad (21)$$

$$\bar{X} = \frac{(1-\epsilon)\, z\, k_s}{V_f\, L^2\, C_{pf}\, \rho_f} \qquad \frac{\eta}{\alpha} = \left(Fo - \frac{z\, \alpha_s\, \epsilon}{V_f\, L^2}\right) \qquad (22)$$

$$\Phi = \frac{1}{2} + \frac{1}{\pi}\int_0^\infty e^{-\bar{X} H_1} \sin\left[\frac{2\eta\beta'}{\alpha} - \bar{X} H_2\right] \cdot d\beta'/\beta' \qquad (23)$$

where

$$H_1 = \frac{2\lambda\,(2\lambda/Bi + HD_1)}{(2\lambda/Bi + HD_1)^2 + HD_2^2} \qquad H_1(\lim\beta'=0) = 0$$

$$H_2 = \frac{2\lambda\, HD_2}{(2\lambda/Bi + HD_1)^2 + HD_2^2} \qquad H_2(\lim\beta'\to\infty) = 0$$

$$HD_1 = \frac{\sinh 2\lambda - \sin 2\lambda}{\cosh 2\lambda - \cos 2\lambda} \qquad HD_1(\lim\beta'\to\infty) = 0$$

$$HD_2 = \frac{\sinh 2\lambda + \sin 2\lambda}{\cosh 2\lambda - \cos 2\lambda} \qquad HD_2(\lim\beta'\to\infty) = \infty \qquad (24)$$

$$\sqrt{\beta'} = \lambda \qquad \lim_{\beta'\to 0} \frac{\sin\left[\frac{2\eta\beta'}{\alpha} - \bar{X} H_2\right]}{\beta'} = \frac{2\eta}{\alpha} - 2\bar{X}$$

This solution was programmed and is shown as plotted in Figure 4. The mathematics were checked independently in the Department of Mathematics at U.B.C. and in addition the solution was checked to converge to that of Anzelius as Bi → 0.

4. Experimental

A sketch of the apparatus used in this study is shown in Fig. 5. The main column, shown in more detail in Fig. 5b, consisted of a 20.3-cm inside diameter stainless steel pipe with a series of welded nipples for inserting thermocouples or pressure taps. The column was wrapped with a copper steam coil (not shown) which could be used to preheat the column to the desired temperature. Temperatures were measured by bare-tipped or sheathed copper-constantan thermocouples which registered temperature readings on a data-logger. Pressure drop measurements were made at room temperature.

Douglas-fir wood chips were obtained from a local supplier, and screened for thickness as recommended by Hatton (10). Classification was done with the following screens:

Top	4 mm round holes
Second	6 mm slotted parallel steel rods
Third	4 mm slotted parallel steel rods
Fourth	2 mm slotted parallel steel rods

Forty to ninety chips from the different cuts were measured for thickness width, and length. The following parameters were determined:

d_p = diameter of sphere of equivalent volume

$$= 2\left(\frac{\text{volume of chip}}{4\Pi/3}\right)^{1/3}$$

ϕ = Sphericity = $\frac{\text{Surface Area of Sphere of Volume Equal to the Chip}}{\text{Surface Area of the Slab-Shaped Chip}}$ (calculated from measured values of chip thickness, width and length)

ρ_c = Density - calculated from dimensions and weight of five carefully measured uniform chips

ε = Bed Voidage - calculated from bed height, volume of cylinder occupied and chip density

Properties of the wood chips and the spherical catalyst particles used for verification of techniques are listed in Table 1; particles are shown in Fig. 6

5. Procedure and Calculation of Heat Transfer Coefficient

The heat transfer experiments were carried out as follows. (Refer to Fig. 5) The outer-shell was preheated via the external coil to the initial temperature which would prevail during the actual heating test before the chips were put in. This temperature was found by a series of trial and error experiments. The object of this step was to avoid transfer of heat from the hot gas to the shell during the early period of heating. As well the walls could not be preheated to too high a temperature or there would be heat transfer from the wall to the gas. Once the wall temperature was at the desired value, and the hot gas was at a steady flowrate and temperature flowing through the by-pass line, (Valve 2 open, Valve 1 closed), the chips were charged to the bed, the walls tapped with a hammer to settle the solids, the thermocouples were inserted, and Valve 1 to the column opened, and the by-pass line (Valve 2) shut.

Then all the temperatures in the packed bed were monitored over time. A typical result is shown in Figure 7. Once the temperature wave had passed through the column, typically 2400s, the experiment was ended.

The thermocouple data, which was followed by the data-logger, was then transcribed to the UBC computer. The mathematical model of heat transfer in the packed bed was used to estimate the heat transfer coefficient, h. This was done by minimizing the sum of $(T_g(z,\theta) - T_{g_{calc}}(z,\theta))^2$ for various assumed values of h. In the usual case, data at 2 bed-depths was used, whereas in some cases temperature data from 3 bed-depths was used. This gave no significant difference in h.

6. Heat Transfer Results

Results for the different experiments are shown as plots of the experimental gas temperatures, and the corresponding calculated values for the gas temperatures using the best fit of the h value. Tables 2 and 3 list the various run conditions covered, and the corresponding values of h which were derived from the results.

6.1 Verification Tests on Spherical Results

Heat transfer tests were first made using spherical catalyst particles in order to compare heat transfer coefficients with values given in the literature. This provided a check on the techniques and apparatus. Figure 8 shows temperature vs. position and time for three values of the Reynolds number. The calculated curves following equations 11 to 13 fitted to give the minimum deviation are also shown. Of the three parameters which define the solution, the Biot number is the only fitted parameter. The thermal properties of the solid were calculated a priori, and all other values were known for the experiment i.e. T, θ, x, η/σ and η. The fitted curves are seen to fit the gas temperature field very well over height to 1-m, and time to 2000 s. The thermal properties, flow conditions and derived coefficients

are listed in Table 2, and the comparison with literature values in Figure 9. As pointed out earlier, in the region of $50 < Re < 2000$, the data from the literature are very widely scattered. Data from the current tests seem to be in good agreement with the previous results. It was concluded from these tests that the techniques used for the heat transfer calculations were valid, and could be used with confidence for the case of wood chips.

6.2 Air to Dry Wood Chip Heat Transfer

Table 3 outlines the conditions for the dry wood chip heat transfer tests. Temperature profiles are shown at two bed depths for the three different wood thicknesses studied, as well as for the mixture of chips. Figure 10a-d shows the thinnest wood chips at four different Reynolds numbers. As the hot air enters it is cooled by the chips, and as the chips are heated the temperature of the gas at any location rises, eventually reaching the inlet temperature as the bed becomes essentially isothermal. As the Reynolds number increases the time for the gas to reach a given temperature decreases e.g. at $Re_p = 255$ the gas temperature reaches 100°C ($T_f = .633\ T_{f_{initial}}$) in about 400 s whereas at $Re_p = 476$, this temperature is reached in about 200 s reflecting the increased heat transfer coefficient between gas and solid.

The model, used to drive the h values, fits very well over the time period. It is noted that generally at low times the temperature rise of the gas is faster than predicted by the model, and at very low times the fit is rather poor. This undoubtedly is due to experimental problems, at the early period of the unsteady state experiment i.e. heat flow effects between wall and bed, and gas and wall, and heat up of the lower part of the vessel below the grid. The fit appears best at the lowest Reynolds number and deteriorates slightly as Re increases.

One experiment was repeated using the 2.44 mm thick chips to give a measure of reproducibility of the method. The derived coefficients were 11.8 W/m^2K for the first run and 12.4 for the second to give an average of 12.1 ± 2.5%. The level of reproducibility is probably somewhat less than this given the potential errors of measurement.

Similar features to those described above for the thin chips are evident with the thicker wood chips - in going from Re_p = 374 to 698 again the time to reach temperature as far as the gas is concerned drops markedly at 0.41-m height. Here the times for 83.3% are 600 s at the lowest Re value, to 350 at the highest gas velocity.

The heat transfer coefficients, as reported in Table 3, also increase with velocity. It should be noted that although the heat transfer coefficients for the larger particles are larger in magnitude than for the thinner chips, the time for the gas to heat-up is generally slower. Similar trends of temperature profile with Reynolds number are noted for the thickest chips - those of 7.3-mm in thickness (Fig. 12) and for the mixture of wood chips of average 4.8 mm thickness (Fig. 13).

In experiments for two different thicknesses, at fixed velocity the temperature profiles were measured both in the gas, and at the center (r_x=0) of given wood chips. Figure 14a and 14b show that for the 2.44 m thick wood chips, at Re_p = 330, the centre-line chip temperature lags the gas temperature by about 12°C near the beginning of heating, 8°C at T_f~ 100°C and 25°C at T_f ~ 110°C. By contrast, with the thicker chip the lag is only 3-4°C over the range of interest. Calculations based on Fig. 2 show that for h = 15 W/m^2K T_o = 120°C this difference should be about ~(1-5)K.

From these measurements we can conclude that in the range of interest

the fitted data for gas temperature can be used to approximate that of the solids within a few degrees. This essentially can save an immense computational job to evaluate the solid temperature from the original model.

6.3 Moist Air to Dry Wood Chip Heat Transfer

The relative increase in heating temperatures of the moist gas typical of that from a Kraft-recovery boiler flue gas, as compared to that of a dry gas is shown for two experiments in Figures 15a and 15b. Here the dimensionless temperature (Tg/Tg_o) is plotted rather than simply Tg. We note that the presence of the moisture, with its condensation onto the solid bed, gives a much increase heat-up time as would be expected. Thus at $Tg/Tg_o \sim .833$ in Fig. 15a the heat-up time drops from 520 s to 210 s which roughly corresponds to an increase of heat transfer coefficient of 2.5 times. A similar effect is noted in Figure 15b for the run with the thickest wood-chips.

6.4 Correlation of Heat Transfer Results

Heat transfer coefficients for the wood chips are plotted versus superficial velocity and versus particle Reynolds number in Figures 16a and 16b. Generally the coefficients increase with Reynolds number, and the 2 and 4 mm thick chip data are virtually identical at a given value of Re. For the larger chips, as mentioned earlier, the coefficient at a given Reynolds number is definitely higher. Figure 17 shows the agreement with literature predictions.

In the present calculation of the heat transfer coefficient h_f, the heat transfer is considered one-dimensional and only the heat entering the broad faces of the chip is considered. Thus for a wood chip of width W, length Y and thickness 2L, the nominal heat transfer area per unit of packed

bed volume is

$$a_{nom} = (1-\varepsilon)\ \frac{2WY}{WY\ 2L} = \frac{1-\varepsilon}{L} \qquad (25)$$

If conduction through the edges is considered the true area for heat transfer per unit volume of bed is

$$a_T = (1-\varepsilon)\ \frac{(2WY + 4WL + 4YL)}{2WYL} \qquad (26)$$

Inserting values for the chip geometries from Table 1 gives:

Average Thickness (mm)	a_{nom} (cm^2/cm^3)	a_T	a_{true}/a_{nom} (-)
2.44	3.58	4.75	1.33
4.03	2.31	3.17	1.37
7.26	1.43	3.70	2.58
4.81	1.973	4.696	2.43

If we take from equation (1) $Q = h_f\ a_{nom}\ (T-t)$

$$= h_T\ a_T\ \ (T-t)$$

then $h_T = h_f\ a_{nom}/a_T$ whence from the data in Table 3, a corrected heat transfer coefficient is obtained. Figure 18 shows the much-reduced scatter in this plot, and the band of values which is then recommended for design purposes. The surface area to be used with this equation then is the true area per unit volume given by equation (26).

It is of interest to examine the expected range of Biot numbers for the current situation. These values are listed in Table 3, and it can be noted that for the thin wood chips Bi < 0.12 which means that essentially the internal thermal resistance may be largely ignored. For the thicker wood chips the Biot modulus becomes significant and reaches values in excess of unity for the thickest chips. Here the dominant thermal resistance lies within the chip. When contacting with wet gas, the coefficient will increase so that internal conduction will dominate the heat transfer process.

7. Pressure Drop Results

Pressure drop measurements were first taken using the spherical catalyst plots to verify the method and techniques. Figure 19 shows excellent agreement (± 2.3% std. dev'n) with the predictions of the accepted Ergun equation.

$$\frac{\Delta P}{\Delta L} = 150 \frac{(1-\epsilon)^2}{\epsilon^3} \frac{\mu V}{(\Psi d_p)^2} + 1.75 \frac{(1-\epsilon)}{\epsilon} \rho_g \frac{V^2}{(\Psi d_p)} \qquad (27)$$

Data for the wood chips are shown in Figures 20a-d. Generally, the Ergun equation predicts smaller pressure drops than were observed. Agreement is best at low pressure drops, and for large particles. The 6-mm chips gave values within ± 1 %, std. dev'n of the Ergun equation values. The reason for the deviation between the accepted equation and the data is not known, but it may be related to the values of the mean diameter and sphericity calculated for the particles. As evident from Table 1, the particles are far from spherical, and the use of the volume/surface mean and sphericity shape factor may not be justified. Figure 21 shows that with fitted sphericity and void fraction the scatter is much reduced.

Figure 22 shows the pressure drop data plotted as a function of velocity for the various wood-chips tested. Within the range of velocities tested this figure gives a direct number for use in design calculations.

8. Conclusions

An unsteady state heat transfer experiment was set up in which hot air at about 130°C was passed through 1-m deep beds of Douglas Fir wood chips. Heat transfer coefficients were calculated from measured temperature profiles using a mathematical model of a packed bed of slabs. The coefficients have been established for a range of velocities and chip thickness. Based on nominal flat-side areas the heat transfer coefficients increased with velocity and with chip thickness. The latter effect appeared to be due to increasing importance of the sides and ends for heat transfer into thicker chips. Basing heat transfer coefficients on the total area, a design chart for the gas to surface heat transfer in heating wood chips has been established. The effect of 30% H_2O in the dry air on heat transfer rates was investigated briefly. Heat transfer rates were about double those in dry air Pressure drop charts are presented for the flow of air through fixed beds of wood-chips. Systematic deviations were found when results were compared to the Ergun equation with measured sphericity and measured voidages. The thickest wood chips fitted the Ergun equation best. Fitted values of sphericity and voidage are presented which permit the Ergun equation to be used within ±9% for all samples. This equation is recommended for velocities outside the range of the design charts.

9. Further work

To establish the basis of the process proposed by Blackwell et al.(2), further information and test work is required:

(i) The heat transfer and mass transfer during condensation needs to be studied to determine the time for heat-up in the case of moisture laden gases.

(ii) A pilot unit should be operated under continuous conditions to prove out the concept in a continuous process.

REFERENCES

1. Blackwell, B.R. et al. "Use of Waste Gases to Preheat Wood Chips in the Pulp and Paper Industry - A Preliminary Survey". Prepared by Beak Consultants Ltd., Vancouver. DSS Contract #)SQ79-00135 Dept. Energy Mines and Resources.

2. Blackwell, B.R., L.E. Harris and J.D. Garshorn "Preheating Wood Chips with Kraft Recovery Boiler Flue Gas", Pulp & Paper Canada 82: 12(1981), p. T432-7.

3. Kunii, D. and J.M. Smith "Heat Transfer Characteristics of Porous Rocks", A.I.Ch.E. J. I, No.1 29 (1961).

4. B.V. Karlekar and R.M. Desmond "Engineering Heat Transfer", West Pulb. Co., St. Paul (1977) Chapt. 4.

5. Anzelius - see C.C. Furnas "Heat Transfer from a Gas Stream to a Bed of Broken Solids - II", Ind. Eng. Chem. 22, No. 7, p. 721-731 (1930).

6. Rosen, J.B. J. Chem. Phys. 20, 387 (1952).

7. Amundson, N.R. "Fixed-Beds with Large Particles - Solid/Fluid Interactions in Fixed and Moving Beds" Ind. Eng. Chem. 48 35 (1956).

8. Siegmund, C.W., Munro, W.D. and N.R. Amundson "Two Problems on Moving Beds", Ind. Eng. Chem. 48 43 (1956).

9. B. Chow "Heat Transfer to Fixed Beds of Wood Chips", M.A.Sc. Thesis, The University of B.C., In Preparation (1985).

10. Hatton, J.V. (Ed.) "Chip Quality Monograph", Chapt. 10, No. 5. In Pulp and Paper Technology Series, TAPPI (1979).

TABLE 1 Properties of Wood Chips and Spherical Particles

Nominal Size	Wood Chips 2-mm	4-mm	6-mm	Mixed	Catalyst Sphere
Sphericity	0.468	0.571	0.643	0.552	1.0
Voidage	0.563	0.535	0.482	0.536	0.445
Density (kg/m^3)	352	352	352	352	801
Avg. Thickness (mm)	2.44	4.03	7.26	4.81	
Deviation (%)	32.8	12.39	27.22	38.6	
Variance	0.0533	0.00403	0.004	0.072	
Avg. Length (cm)	3.39	2.54	3.63	3.93	
Deviation (%)	37.8	18.4	37.5	40.1	
Variance	2.55	0.094	3.58	4.73	
Avg. Width (cm)	0.964	1.881	1.842	1.564	
Deviation (%)	46.4	12.5	26.7	35.9	
Variance	0.272	0.0478	0.377	0.437	
Avg. Diameter (cm)	1.045	1.53	2.007	1.632	0.476

TABLE 2 A Summary of Heat Transfer Run Conditions and Results for Spherical Particles

Run No.	Sphere Diameter (mm)	Air Flow $(m^3/s)x10^3$	Init. Air Temp (°C)	Velocity m/s	h_f W/m^2K	Re*	Nu*	Bi	Cp J/kg°K
3	4.78	1.09	133.	0.336	67.6	87	10.15	0.054	1795
2		2.2	139.5	0.6775	83.6	169.	12.55	0.066	1795
2		3.3	129.0	1.018	110.31	228.	16.56	0.088	1795
2		2.2	139.5	0.6775	81.02	169.	12.16	0.065	1773
3		3.3	129.0	1.018	103.1	228.	15.48	0.082	1814

* Calculated at 100°C

Note: All the h_f values were calculated with fitted k_s = 2 W/mK because there was no practical difference between results using k_s (estimated) 2.5 W/mK and k_s (fitted) of 2

TABLE 3 A Summary of Heat Transfer Run Conditions and Results for Wood Chips

Run No.	Chip Thickness (mm)	Air Flow* $(m^3/s)x10^2$	Init. Air Temp (°C)	Velocity* m/s	h_f W/m^2K	Re_p*	Nu*	Bi
2	2.44	1.93	117	..594	12.3	255	4.037	0.16
2		2.48	123	.766	14.8	329	4.850	0.192
3		3.04	125	.938	15.9	403	5.21	0.206
3		3.60	131	1.11	17.0	476	5.58	0.221
2	4.03	1.93	111	.594	11.8	374	5.67	0.253
1		1.93	115	.594	12.4	374	5.96	0.266
2		2.48	123	.766	17.5	483	8.47	0.325
2		3.04	126	.938	20.	590	9.61	0.429
2		3.60	129	1.11	23.4	698	11.24	0.503
2	7.26	1.93	116	.594	31.8	491	20.04	1.23
2		2.48	121	.766	33.7	633	21.24	1.301
2		3.04	127	.938	42.0	774	26.47	1.622
2	4.81	1.93	116.5	.594	16.0	399	8.21	0.409
2	mixed	3.04	128.5	.938	33.1	630	17.0	0.845

* Calculated at 100°C

k_s (Dry) = .094 W/m K C_{ps} = 2.516 kJ/kg K

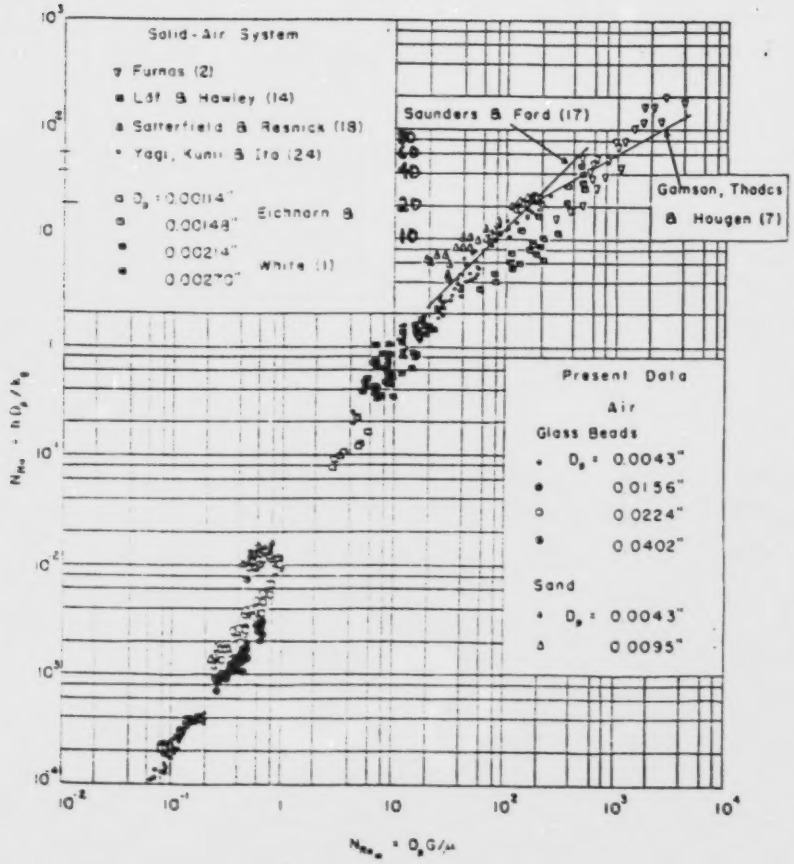

Fig. 1 Literature Heat Transfer Data for Particles in Packed Beds

Source	Particle Size Range	Material
Furnas	0.3 - 7.6 cm	ores, coke
Lof and Hawley	0.48 - 3.81 cm	gravel

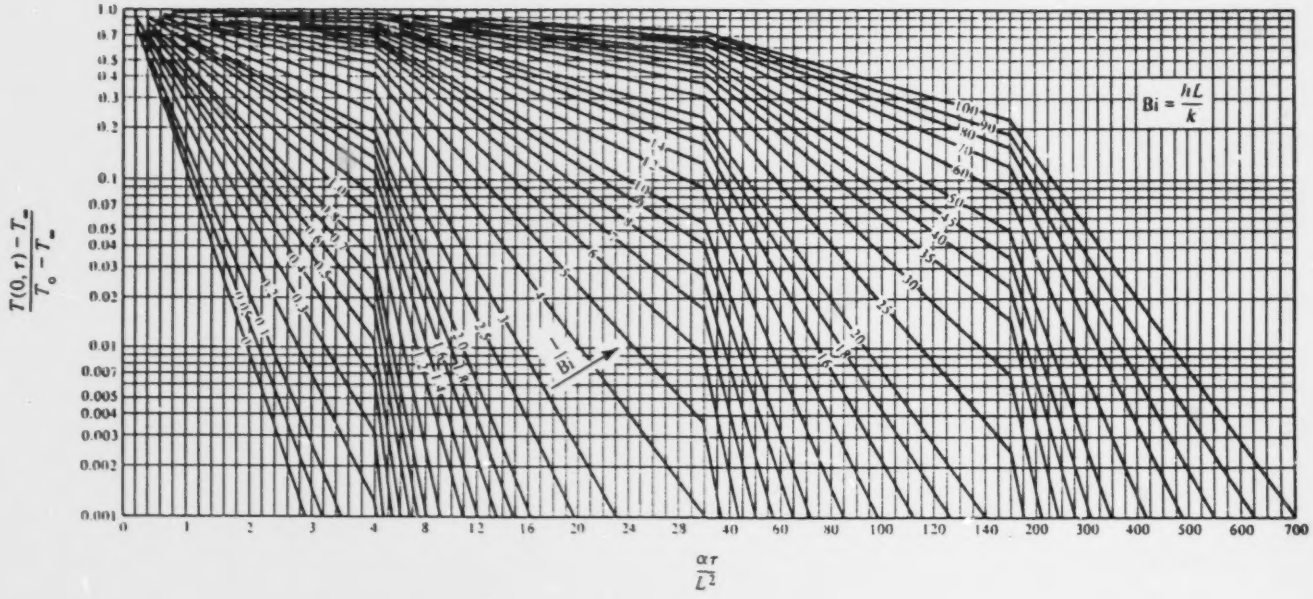

Centerline temperature for a slab of thickness, $2L$

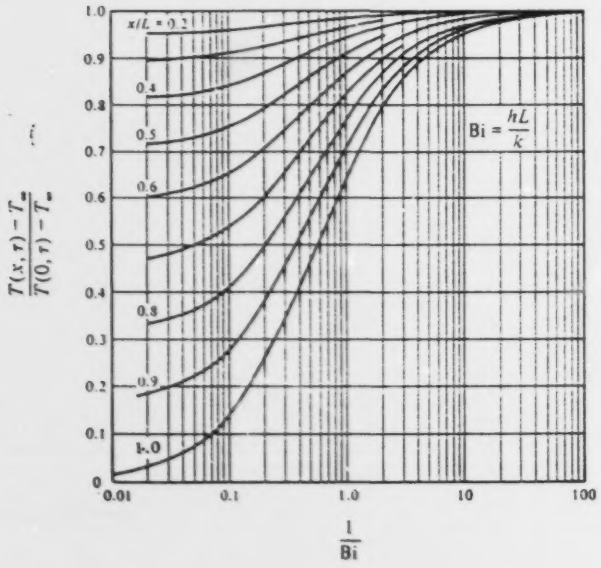

Temperature as a function of centerline temperature in a slab of thickness, $2L$

Fig. 2 Single Particle Internal Conduction Solutions

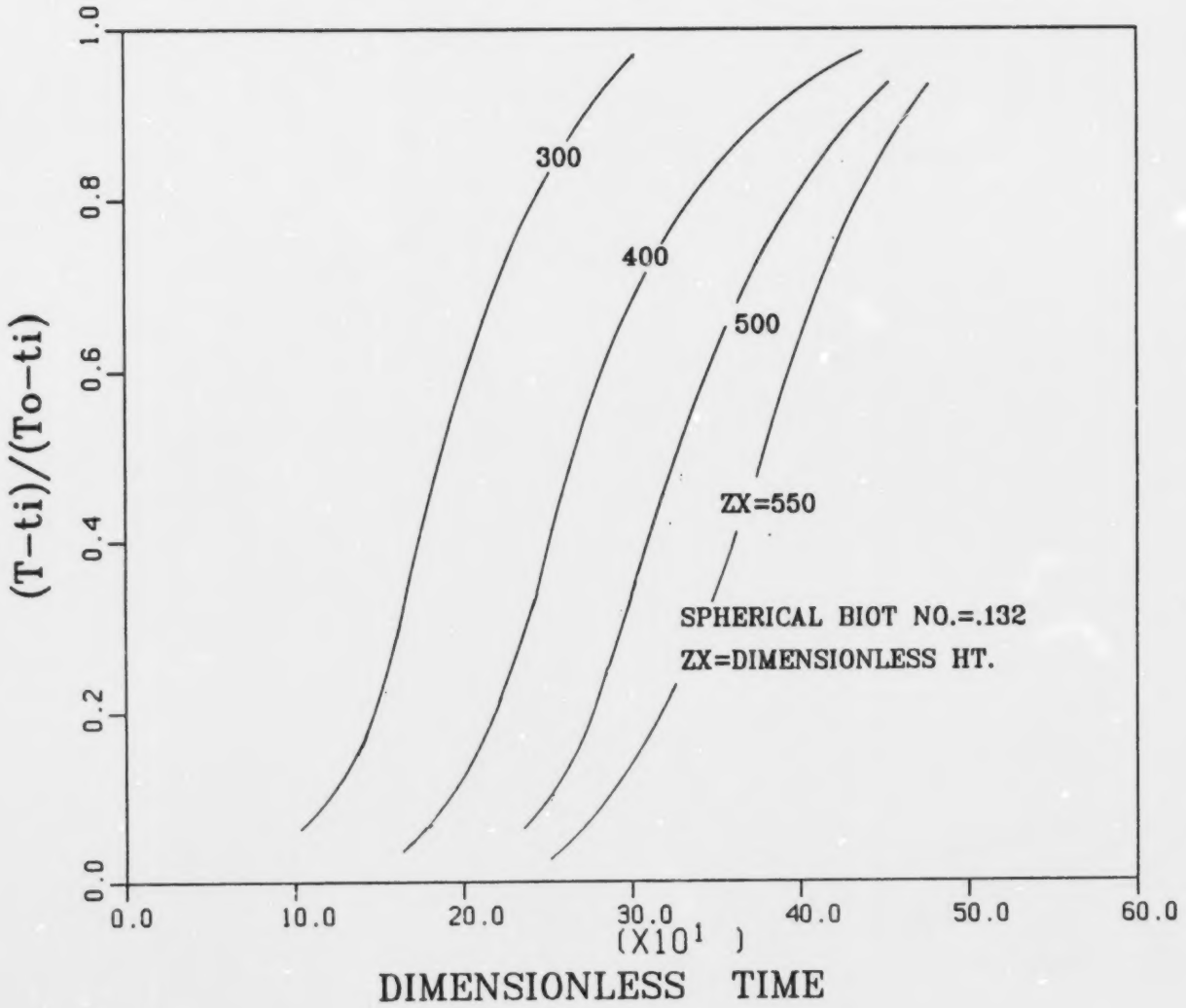

3. Theoretical temperature profiles for a bed of spheres

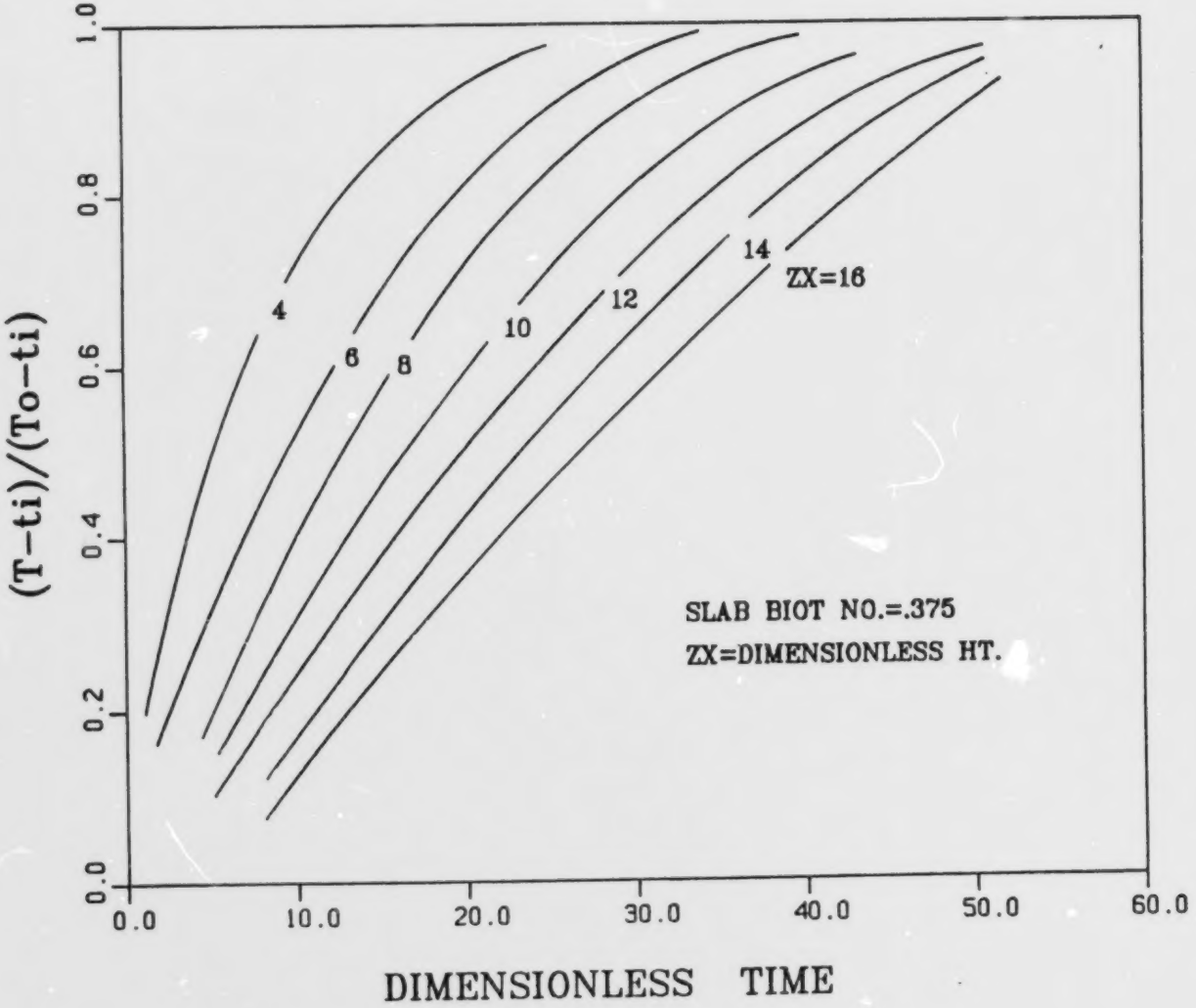

Fig 4. Theoretical temperature profiles for a bed of slabs

Fig. 5a Schematic of Apparatus

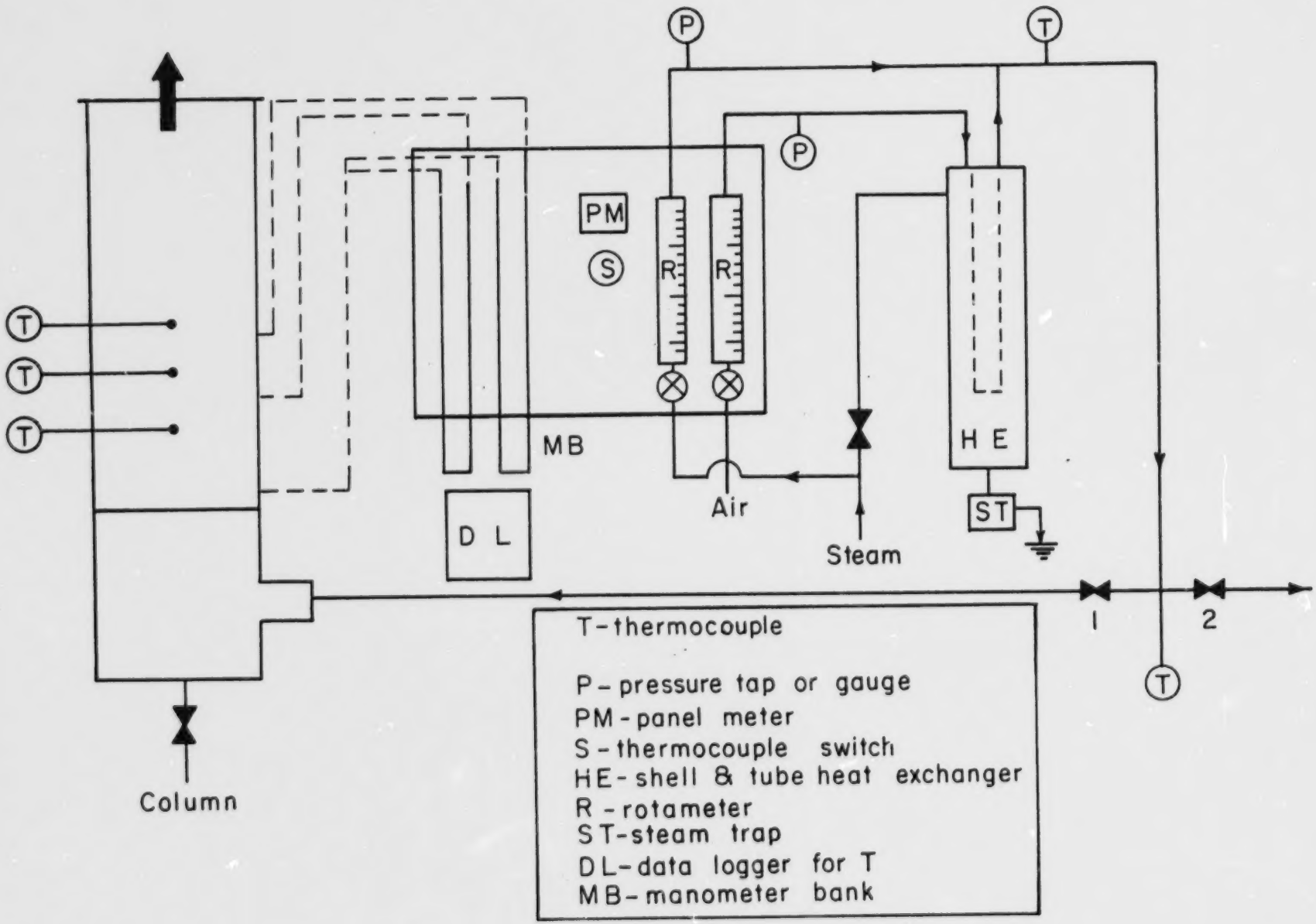

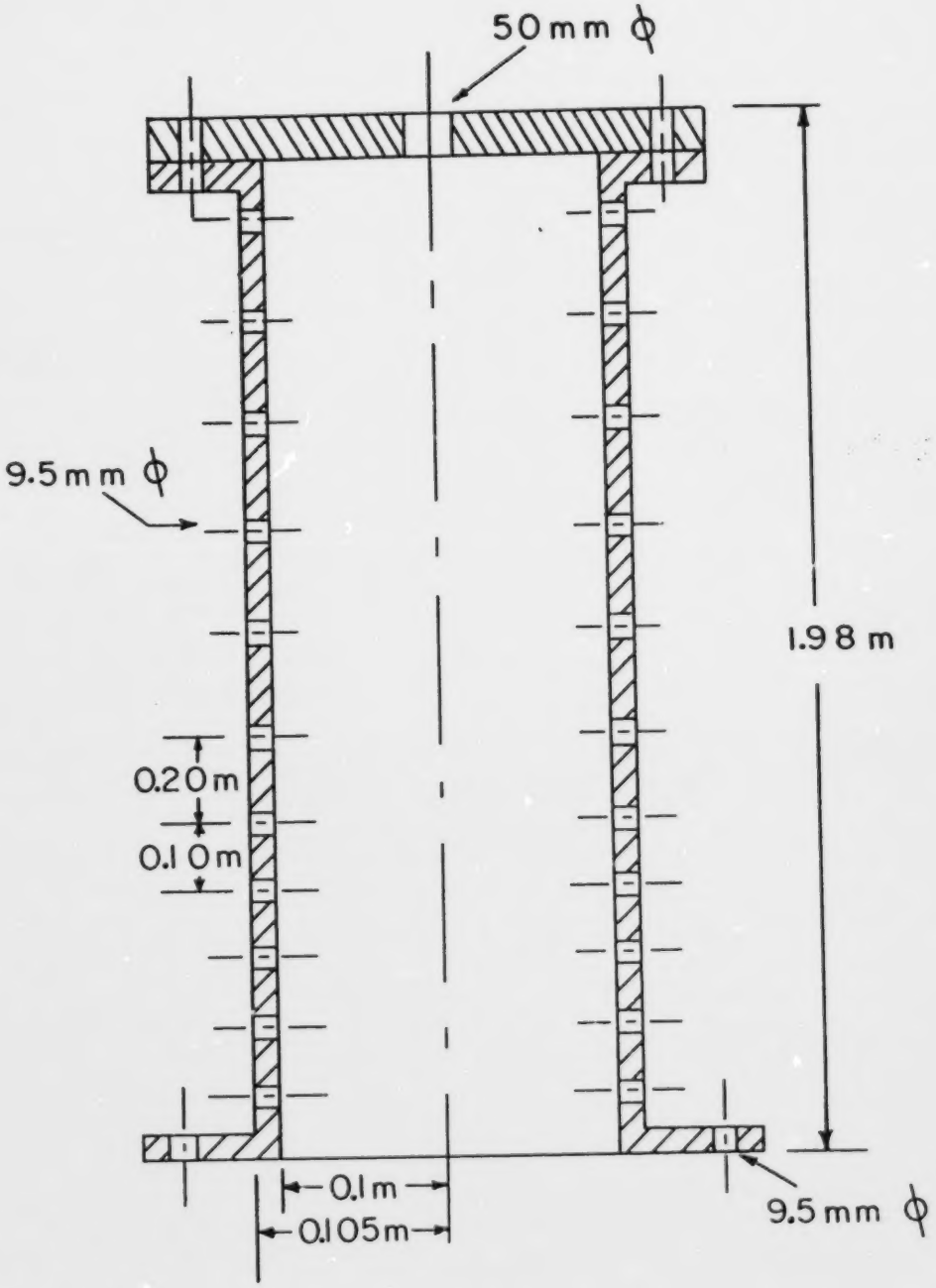

Fig. 5b Details of Main Column

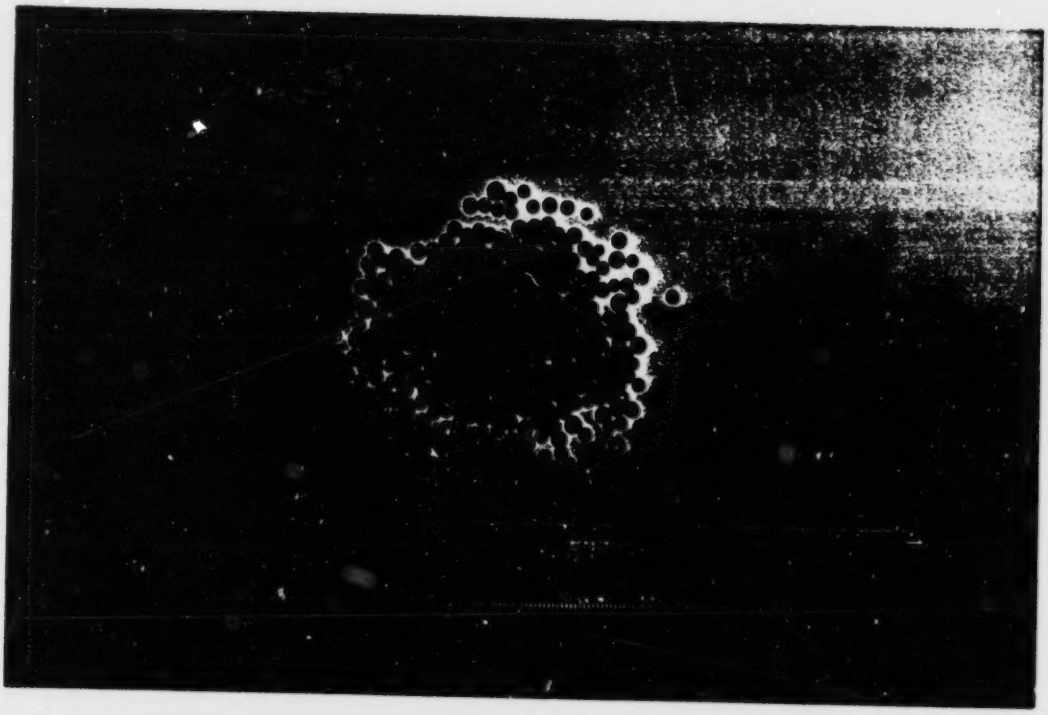

Fig. 6a Spherical Catalyst Particles

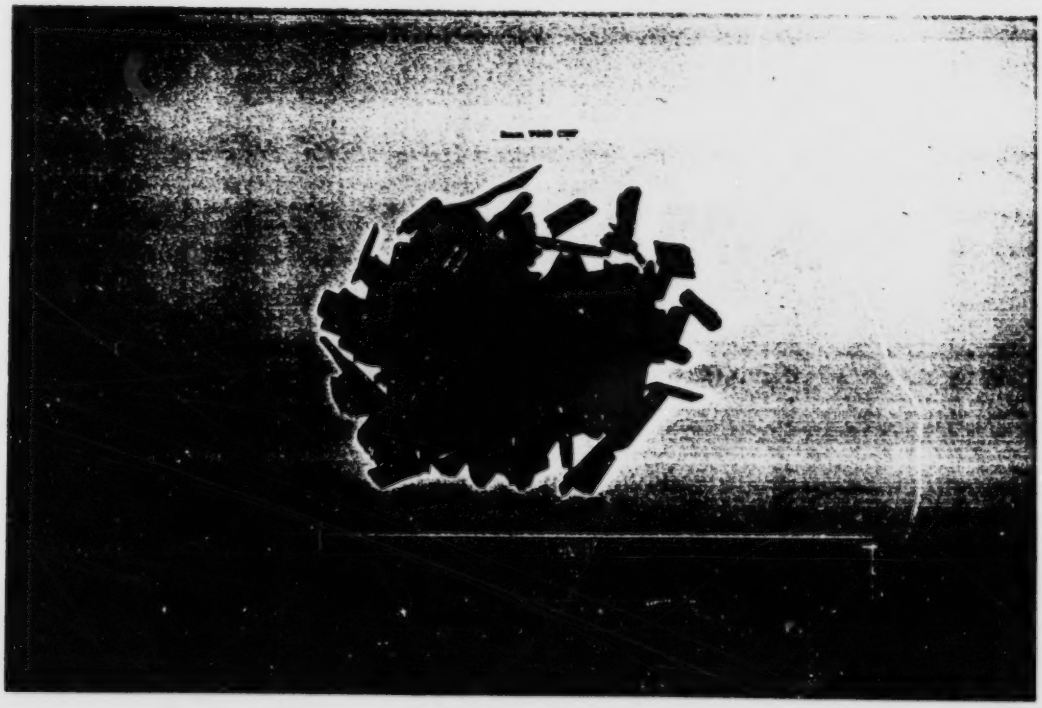

Fig. 6b Nominal 2-mm Thick Wood Chips
(Average thickness 2.44 mm)

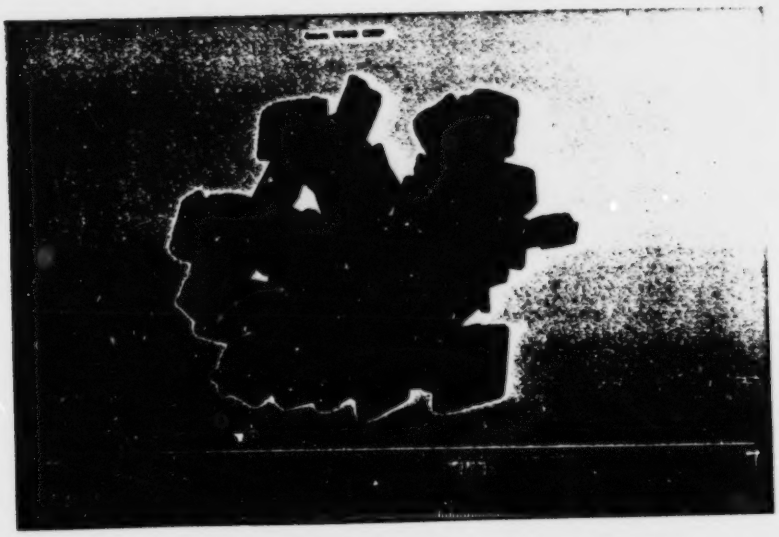

Fig. 6c Nominal 4-mm Thick Wood Chips (Average Thickness 4.03 mm)

Fig. 6d Nominal 6-mm Thick Wood Chips (Average Thickness 7.26 mm)

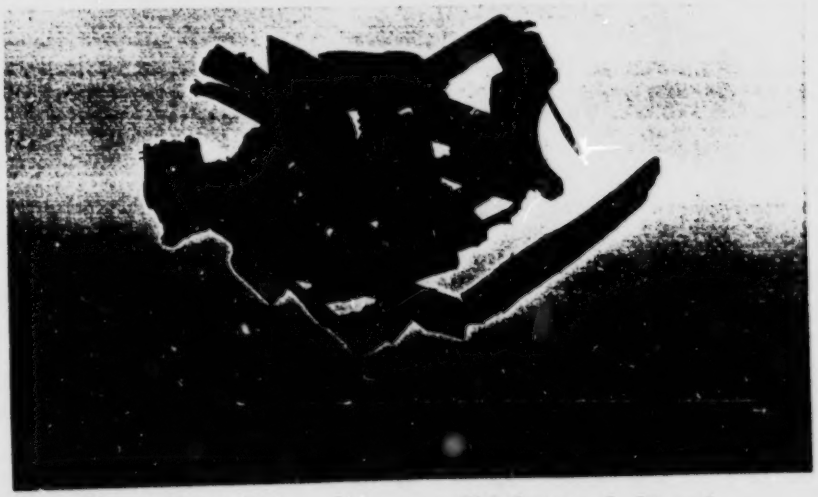

Fig. 6e Mixed Wood Chips (Average Thickness 4.81 mm)

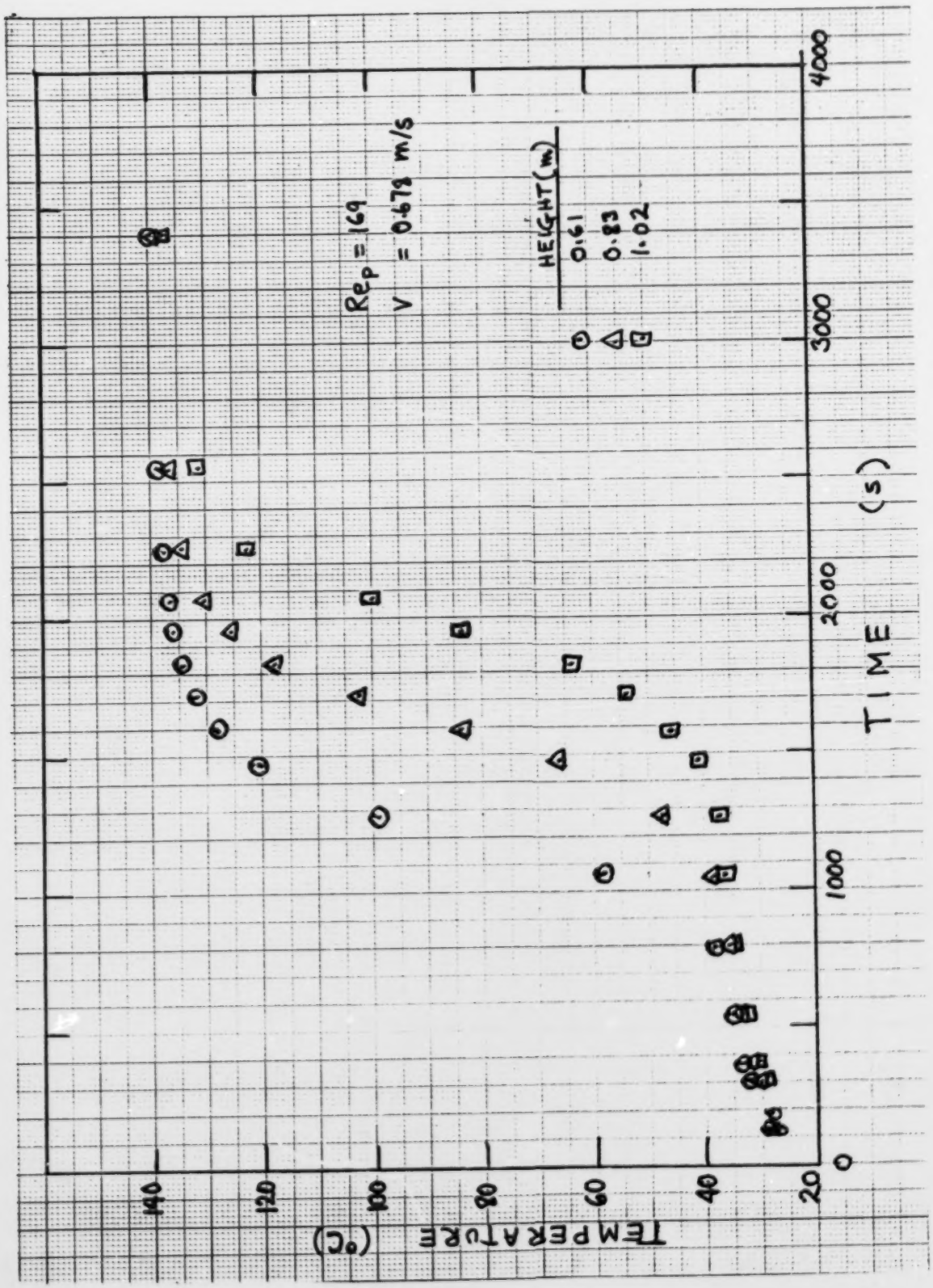

Fig. 7 Typical Result of Raw Temperature versus Time Data for Spherical Particles

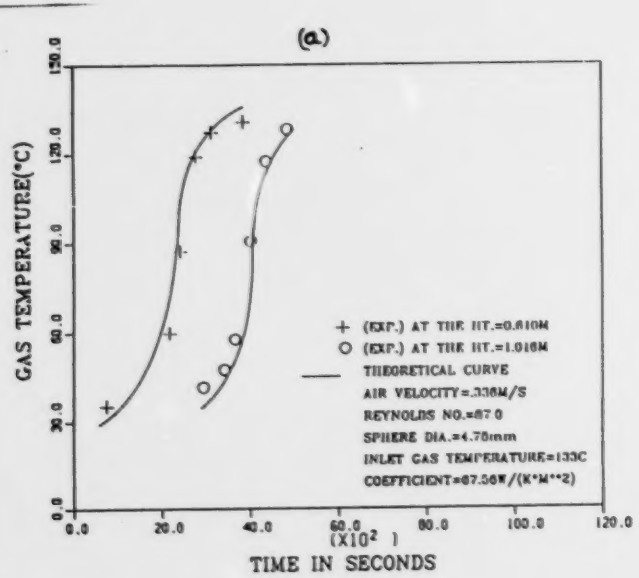

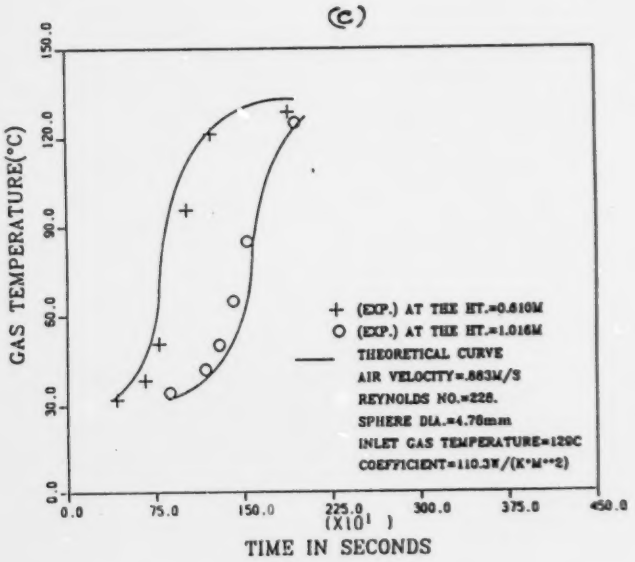

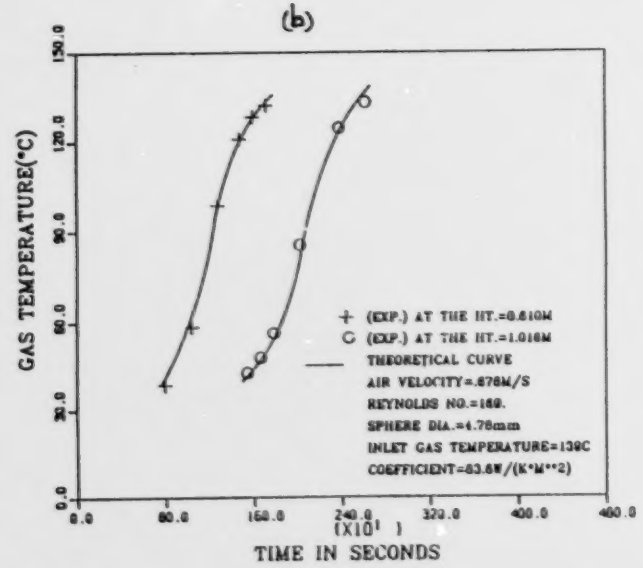

8. Temperature profiles for spheres at a) Re_p = 87 b) Re_p = 169 and c) Re_p = 228

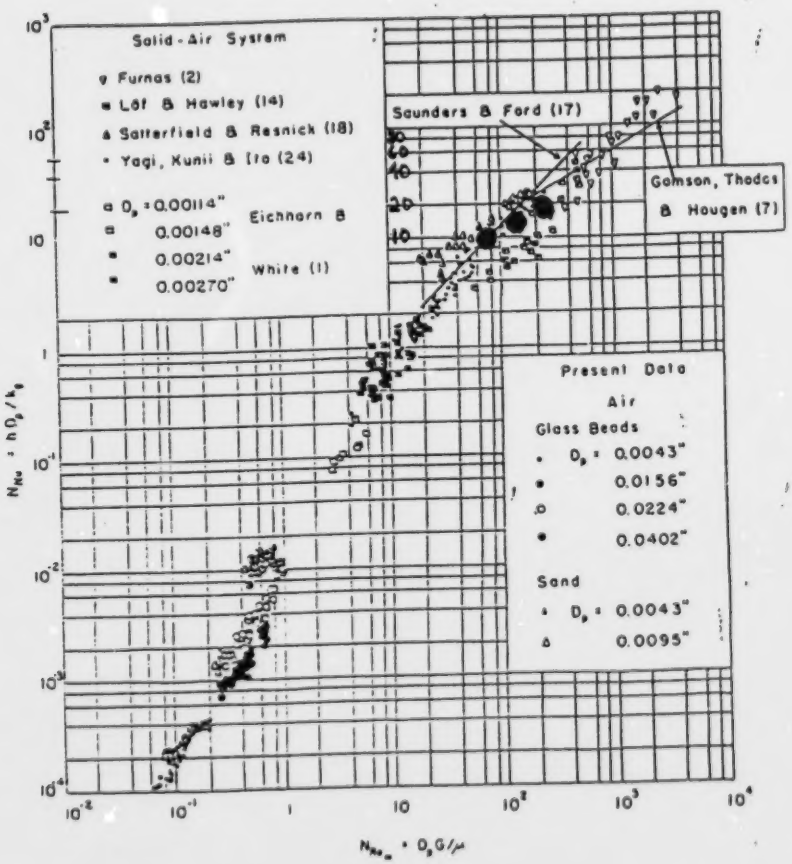

Fig. 9 Comparison of Spherical Particle Data with Literature Values (● This study)

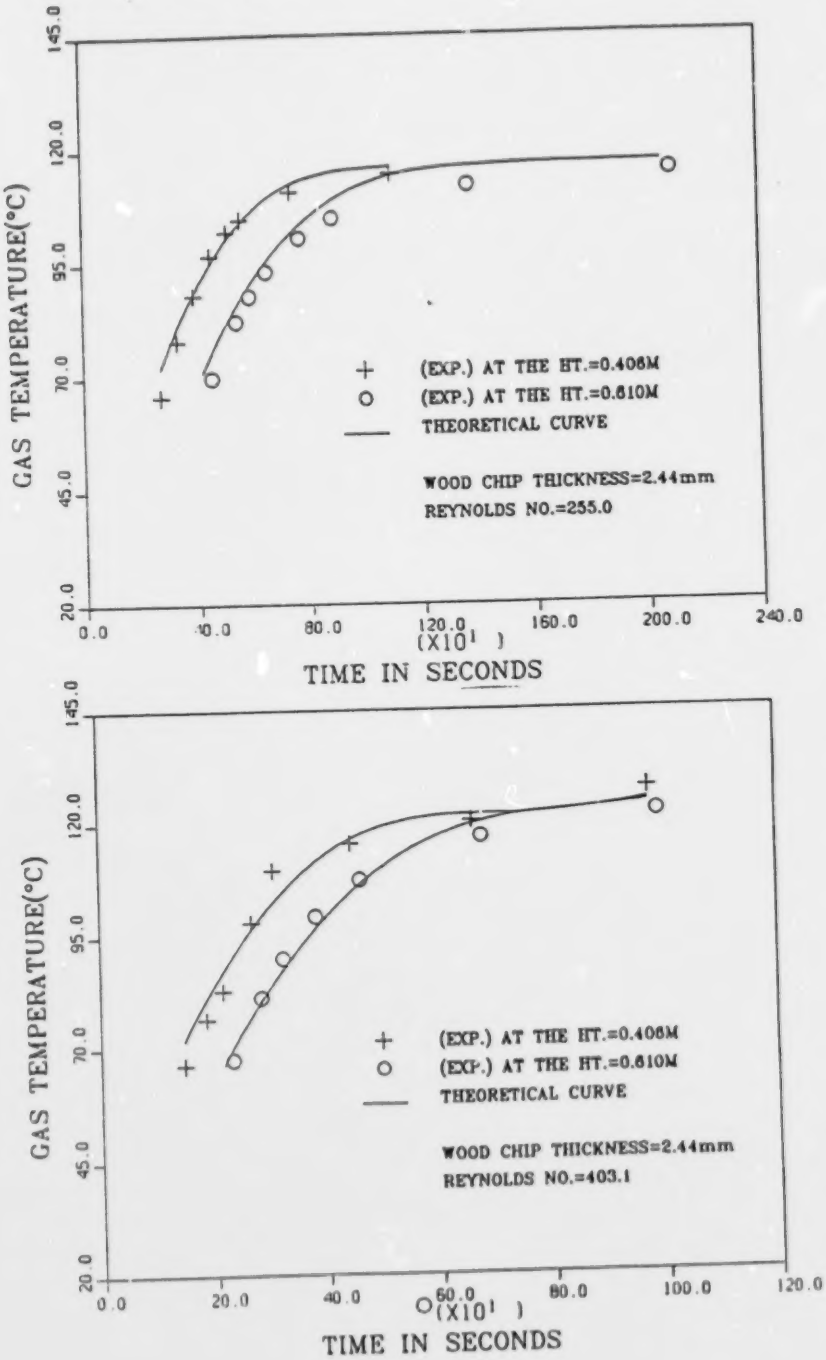

Fig. 10 Temperature Profiles for 2.44-mm Thick Wood Chips
a) Re_p = 255 b) Re_p = 403

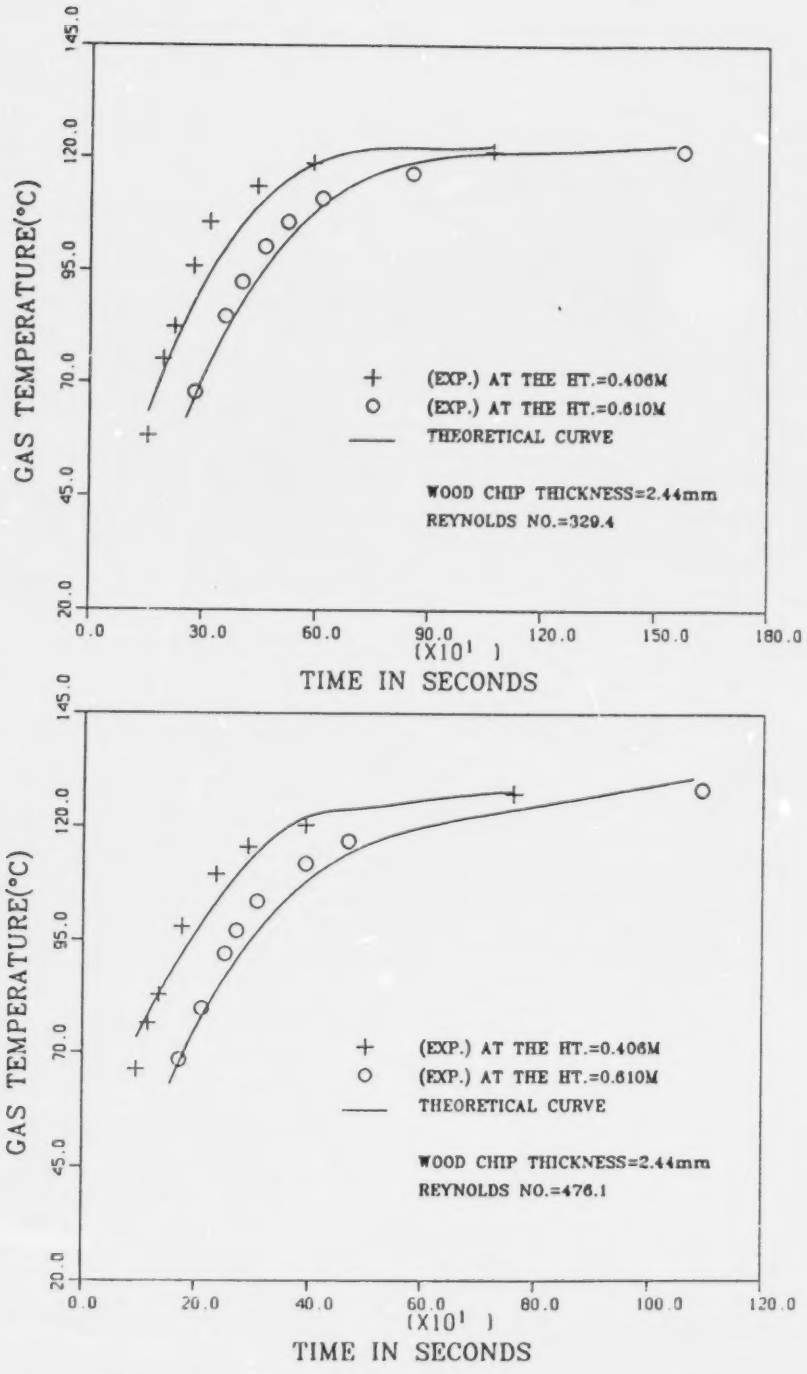

Fig. 10 Temperature Profiles for 2.44-mm Thick Wood Chips
c) $Re_p = 329$ d) $Re_p = 476$

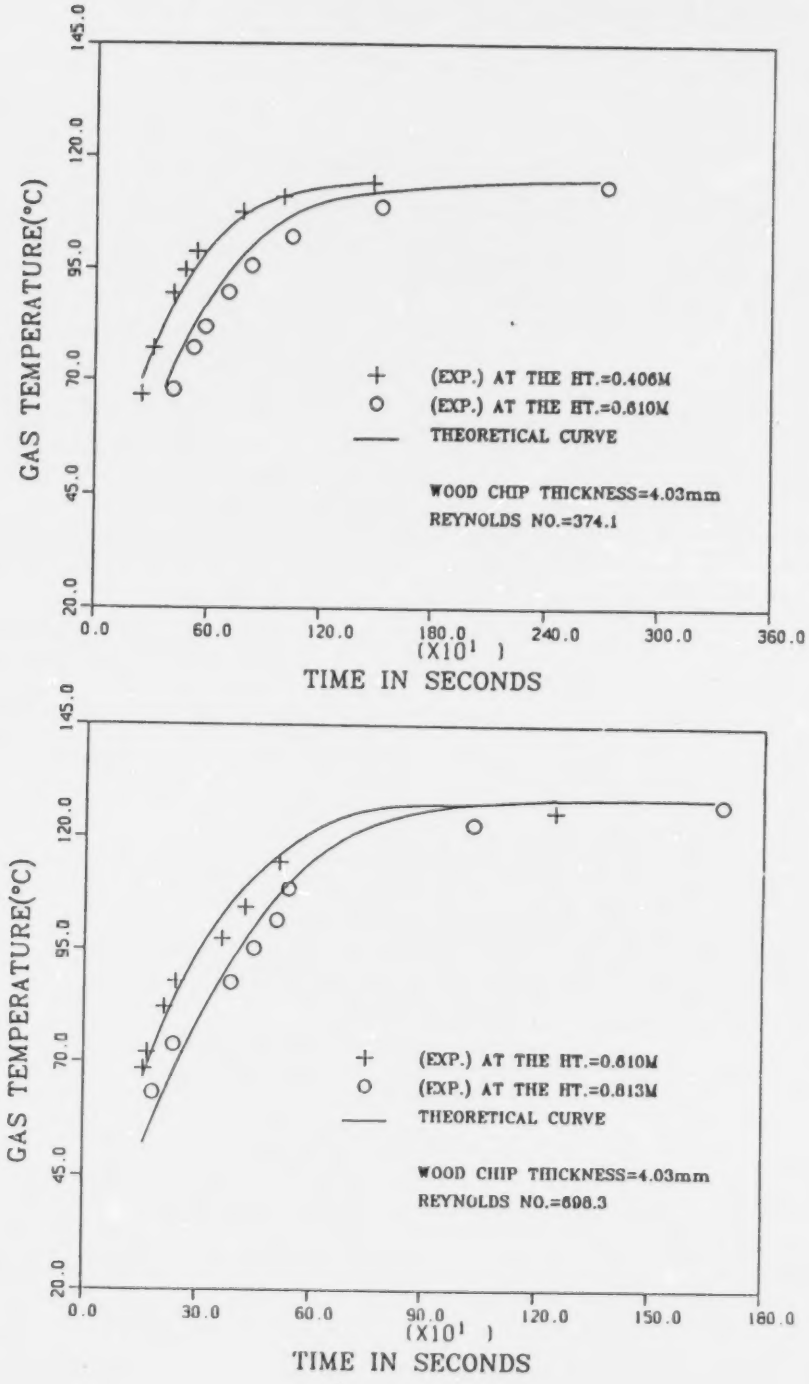

Fig. 11 Temperature Profles for 4.03-mm Thick Wood Chips
a) Re_p = 374 b) Re_p = 693

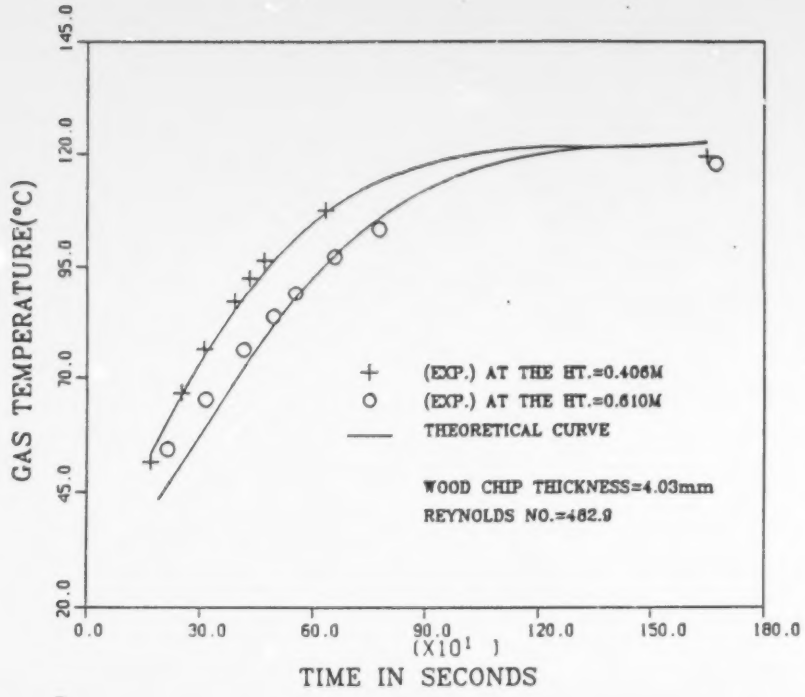

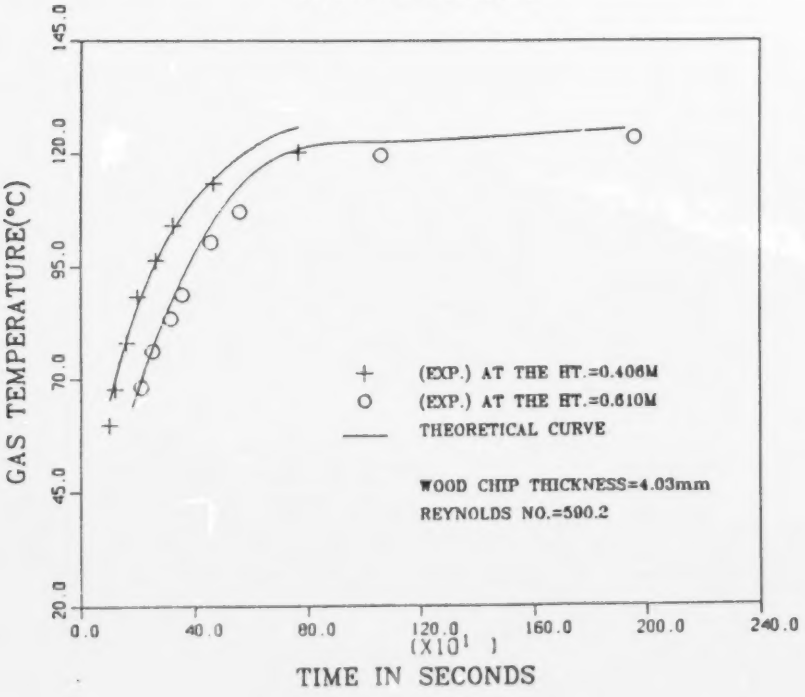

Fig. 11 Temperature Profiles for 4.03-mm Thick Wood Chips
c) Re_p = 482 d) Re_p = 590

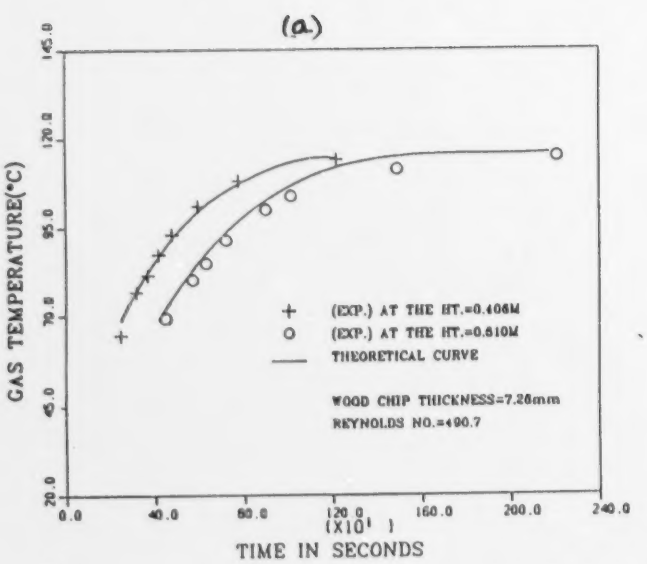

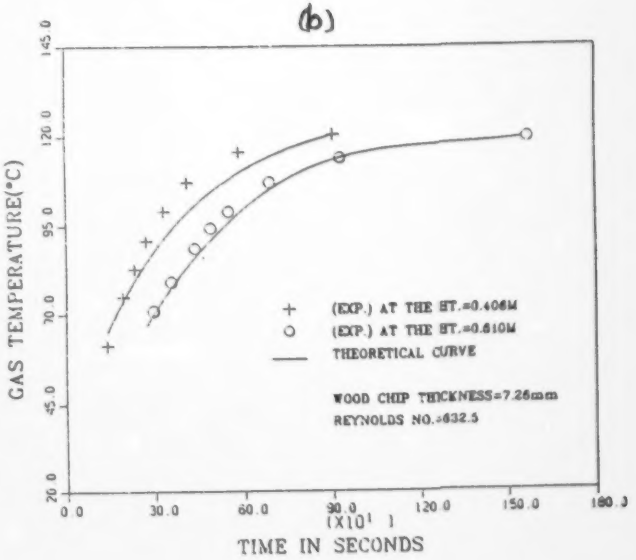

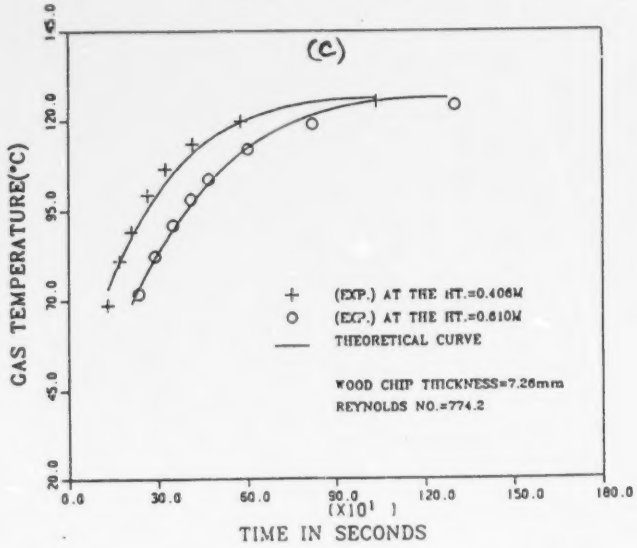

Fig. 12 Temperature Profiles for 7.26-mm Thick Wood Chips
a) Re_p = 491 b) Re_p = 633 c) Re_p = 774

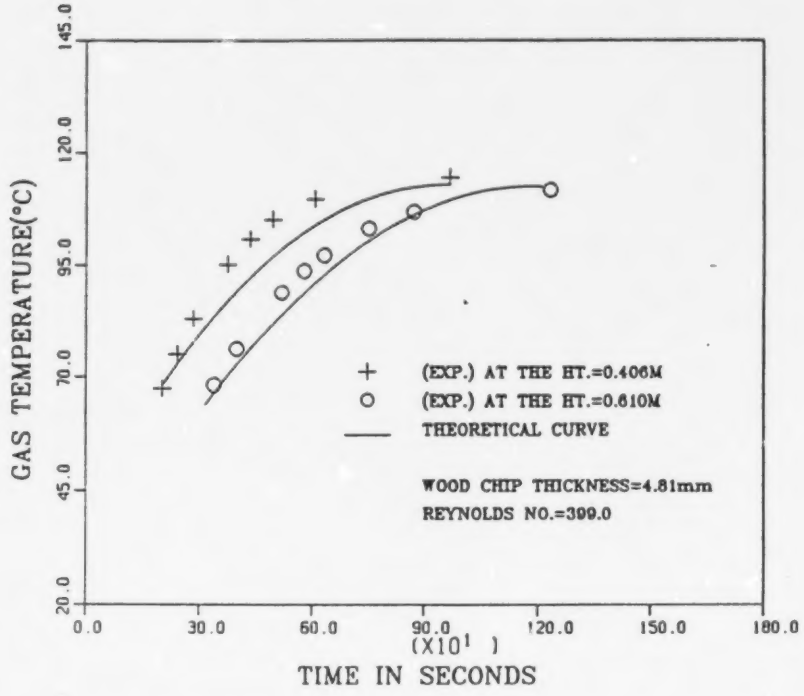

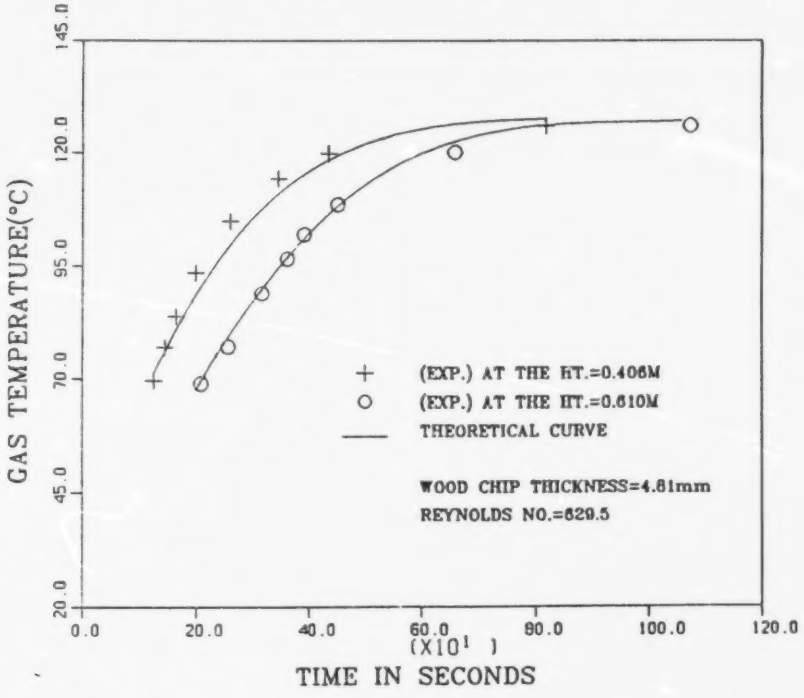

Fig. 13 Temperature Profiles for Mixed Wood Chips
a) Re_p = 399 b) Re_p = 630

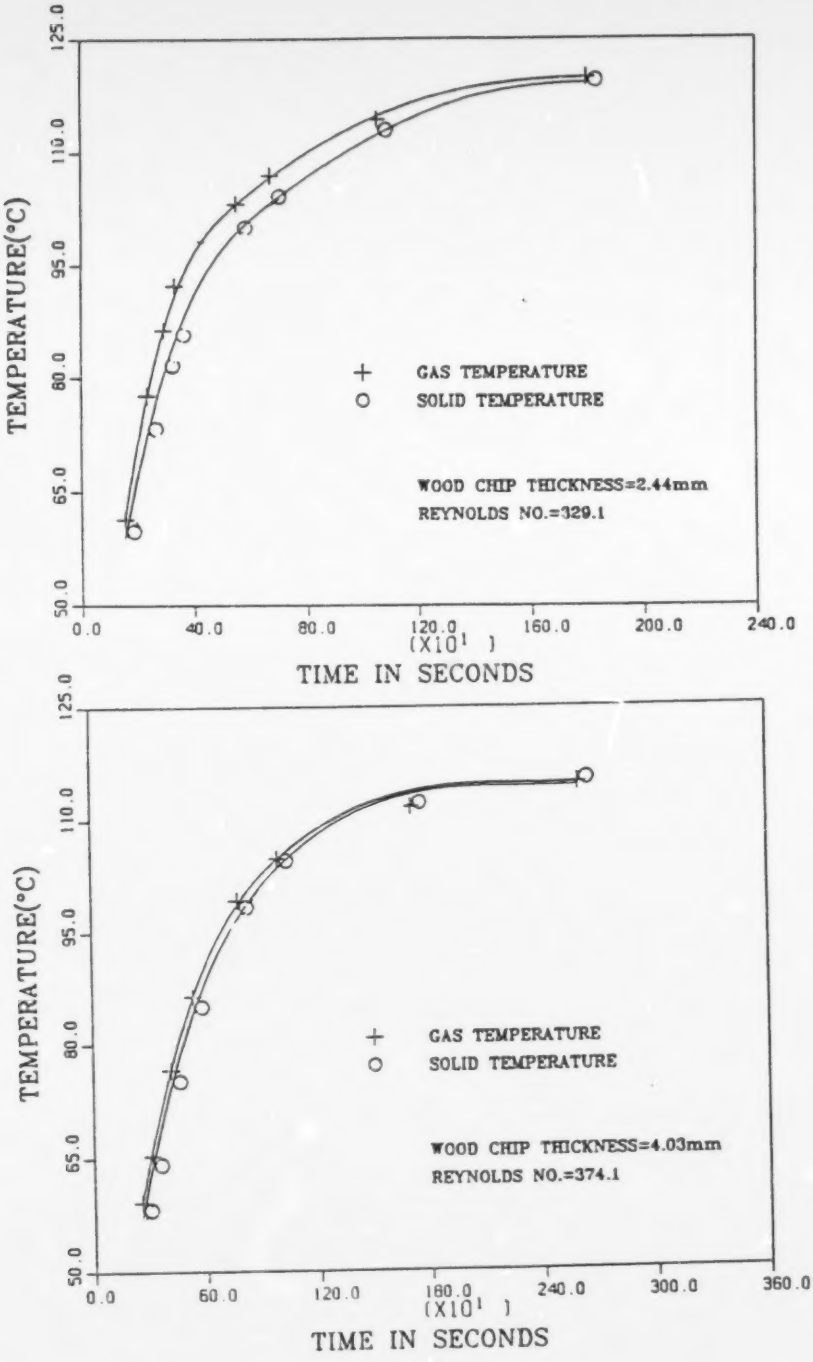

Fig. 14 Internal Wood Chip and Air Temperature for
a) 2.44-mm Thick Wood Chip b) 4.03-mm Thick Wood Chip

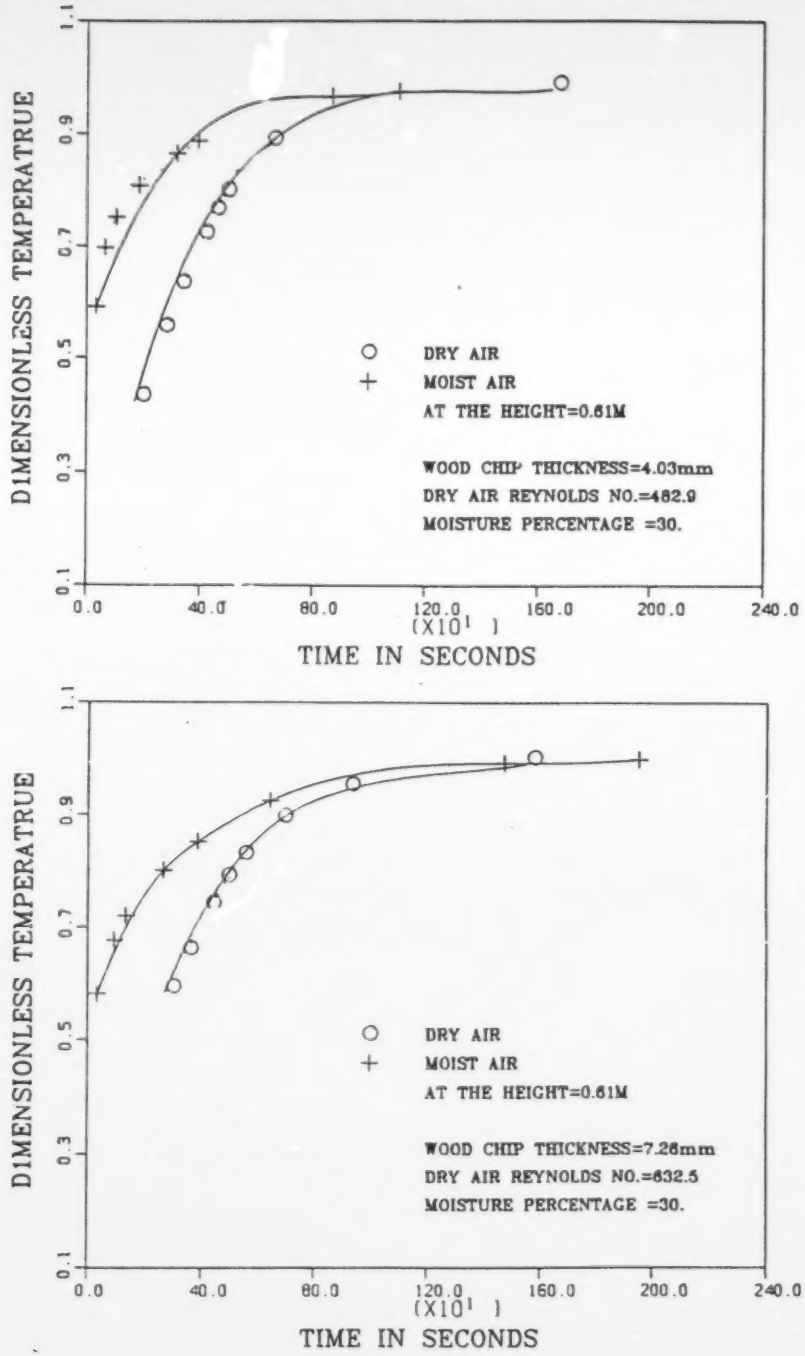

Fig. 15 Comparison of Temperature Profiles for Dry Air and Air - 30% H_2O Mixture a) 4.03-mm Thick Wood Chip b) 7.26-mm Thick Wood Chip

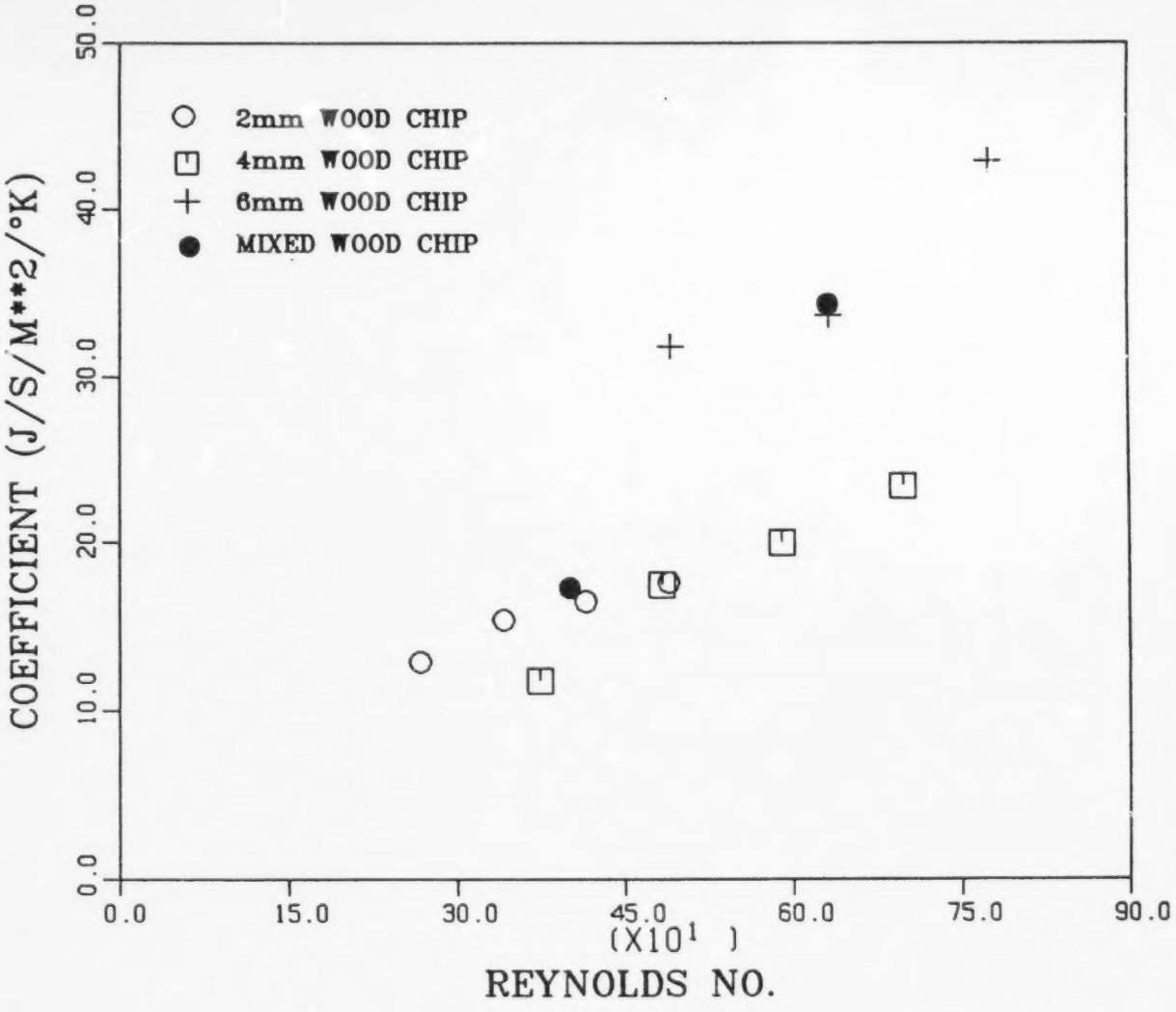

Fig. 16 Correlation of Heat Transfer Coefficient with Reynolds Number

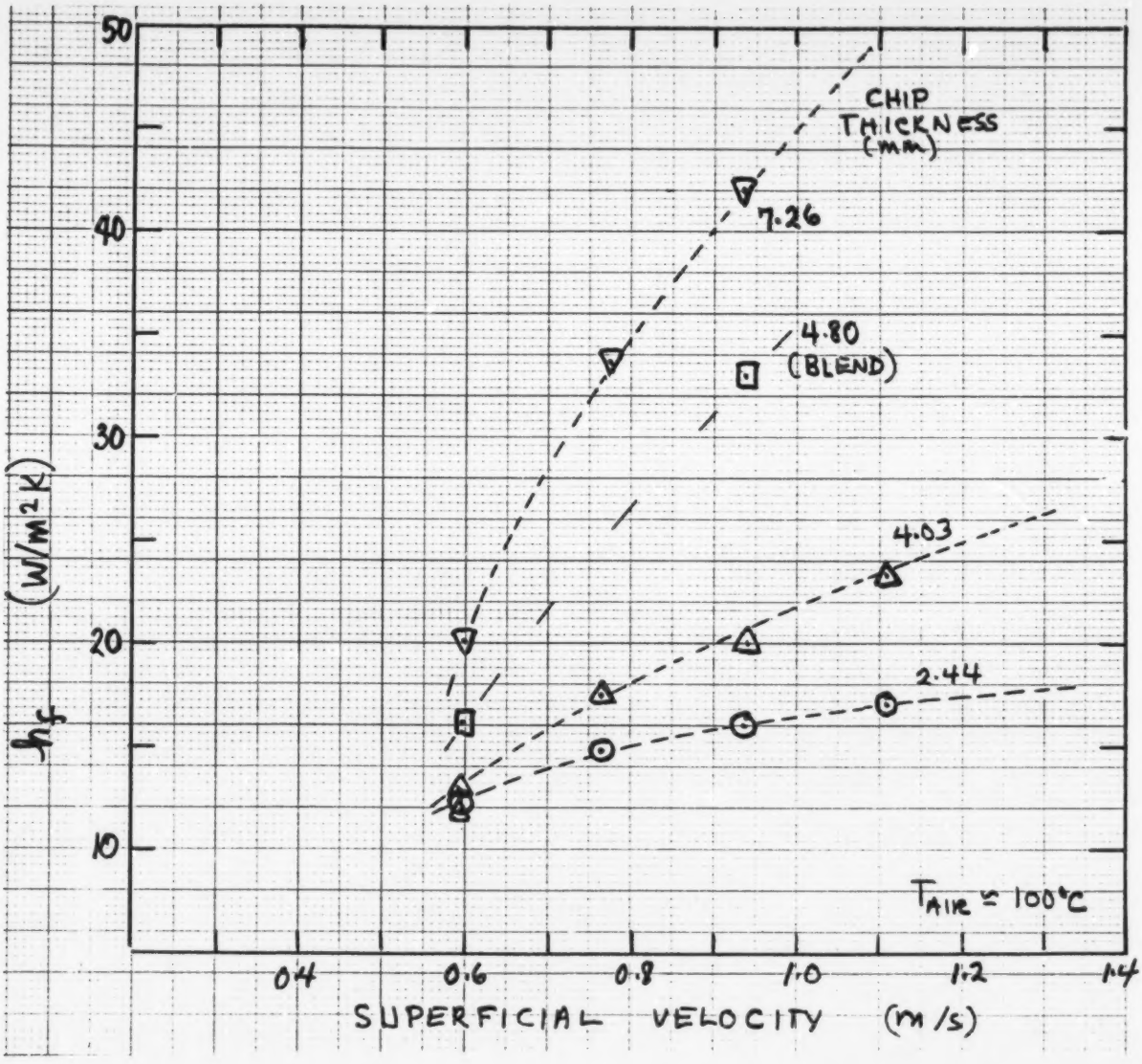

Fig. 16b Plot of h_f versus Superficial Velocity

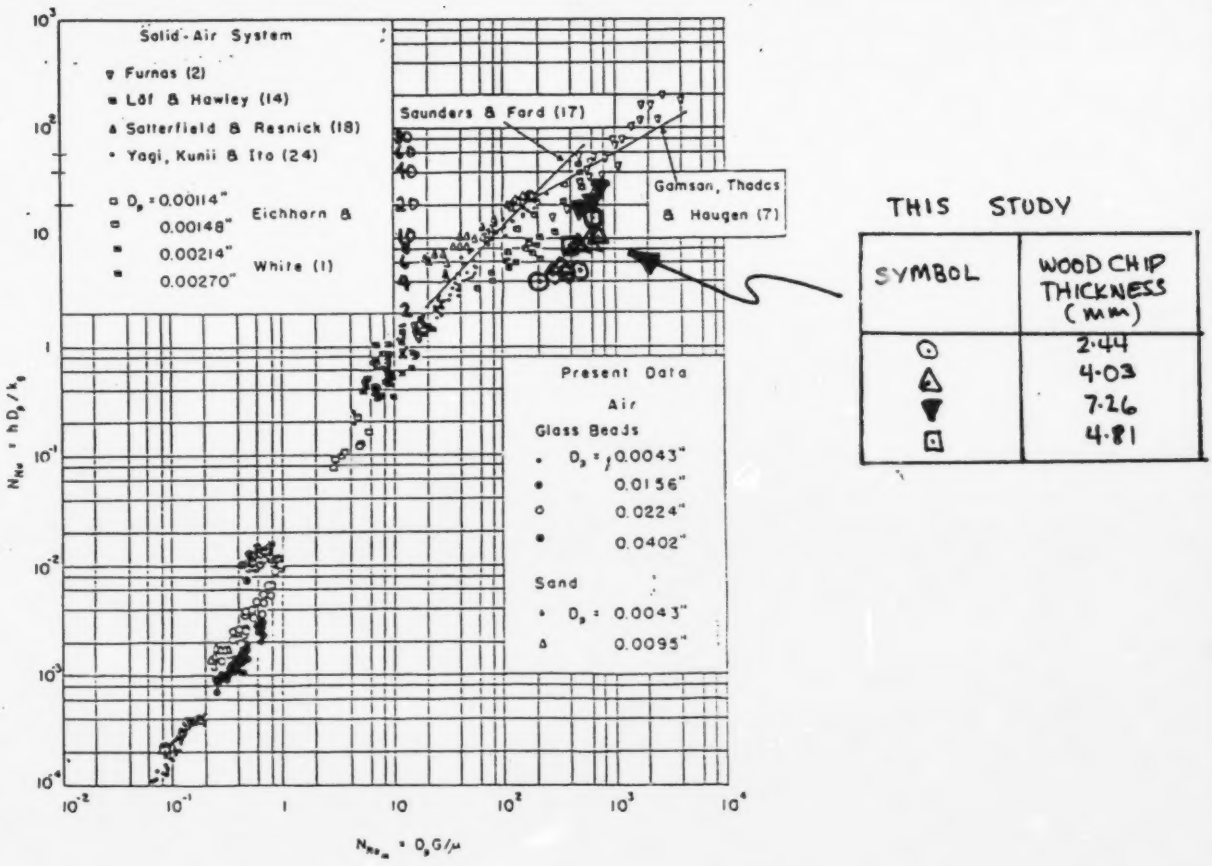

Fig. 17 Comparison of Wood Chip Data with Data for Other Solids

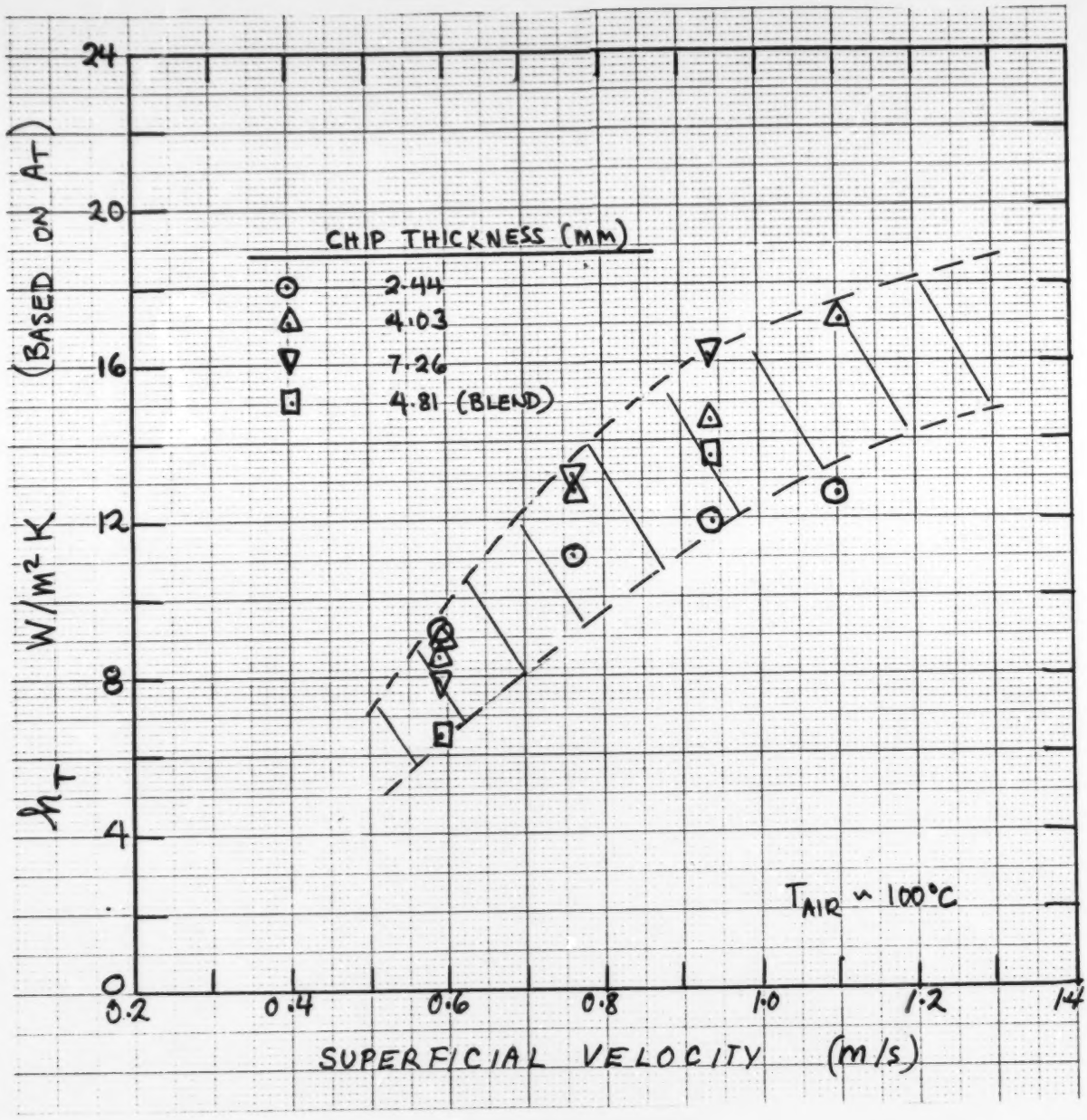

Fig. 18 Plot of h_T versus Superficial Velocity

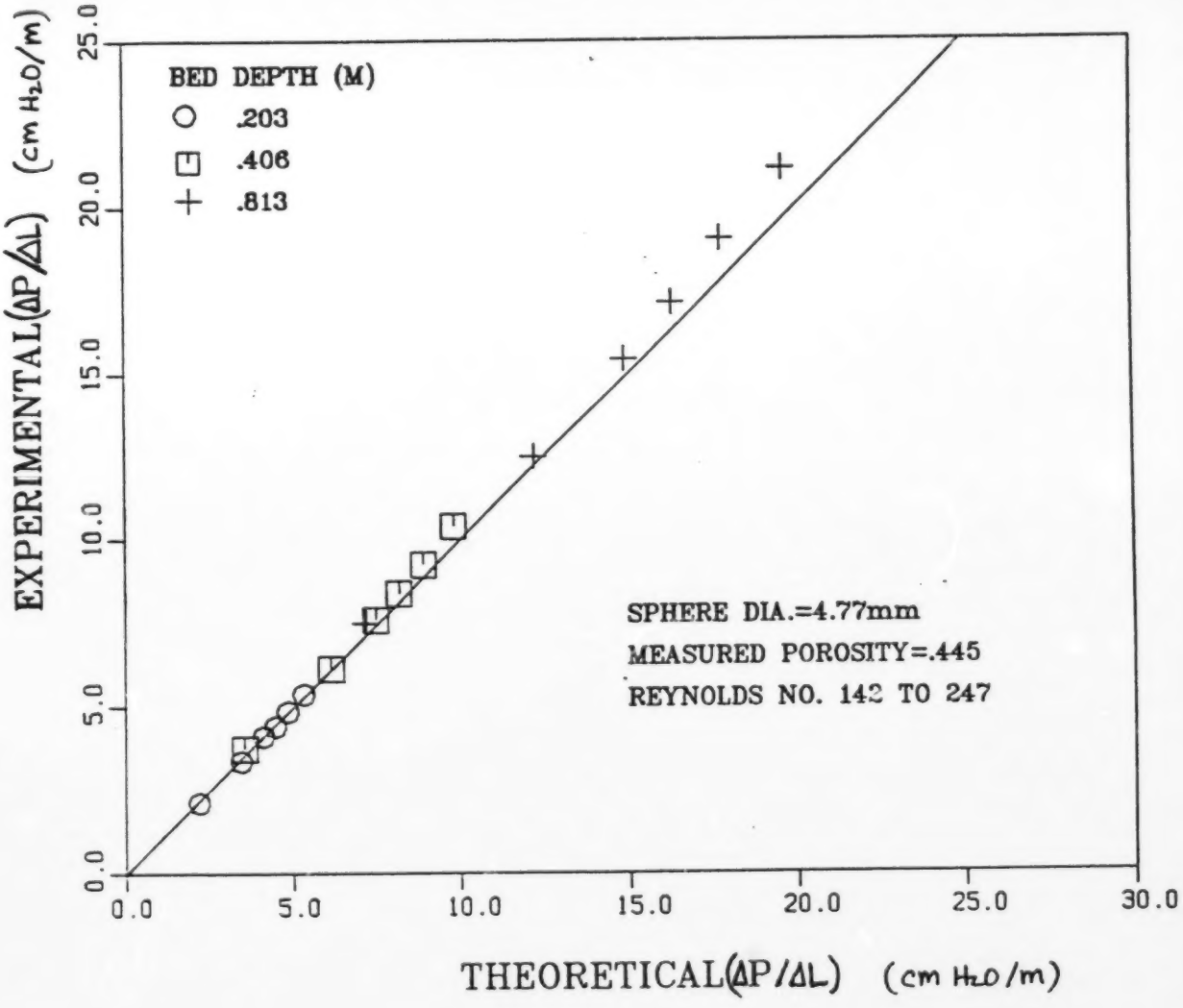

Fig 19. Pressure drop data for spherical particles

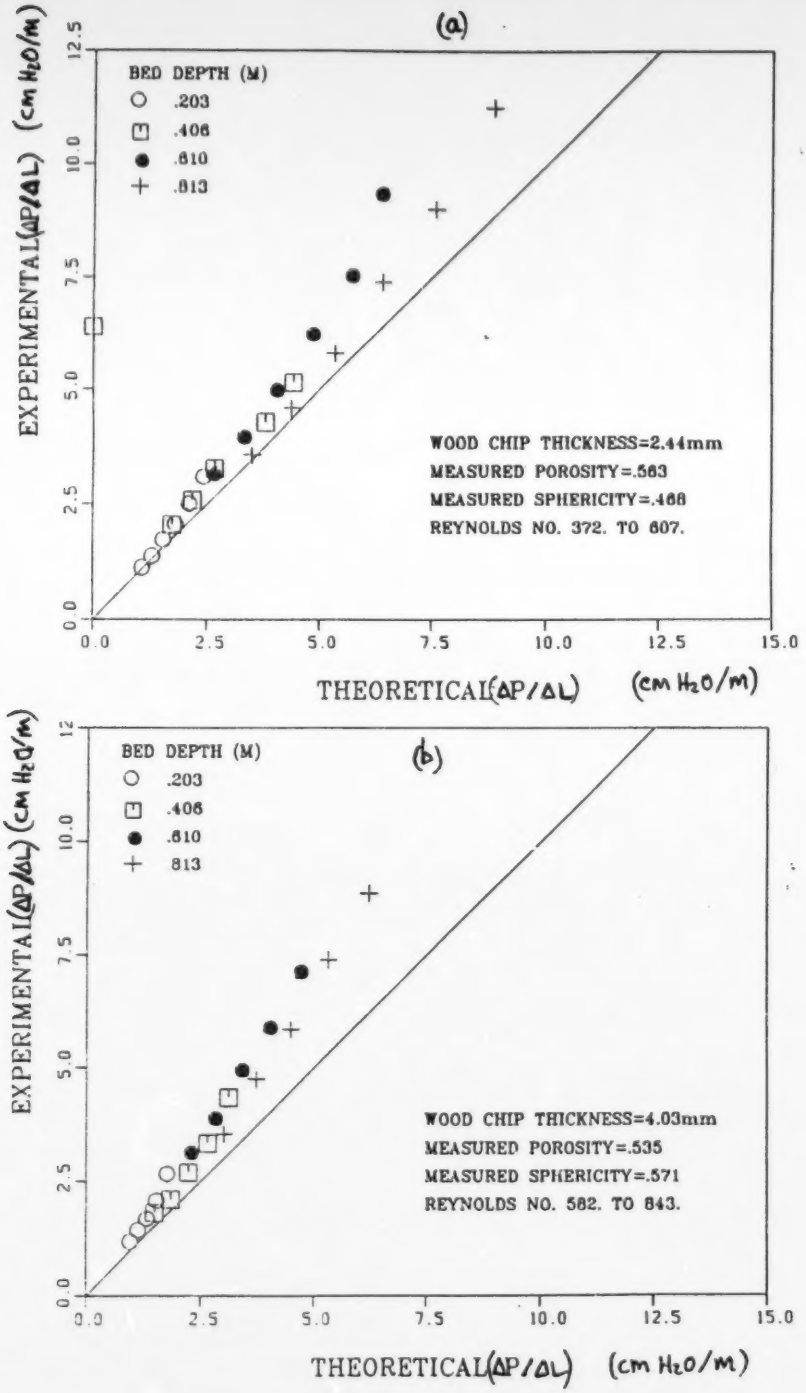

20. Experimental pressure drop versus Ergun equation prediction for wood chips of thickness
a) 2.44-mm b) 4.03-mm c) 7.26-mm d) 4.8 mm (mixed)

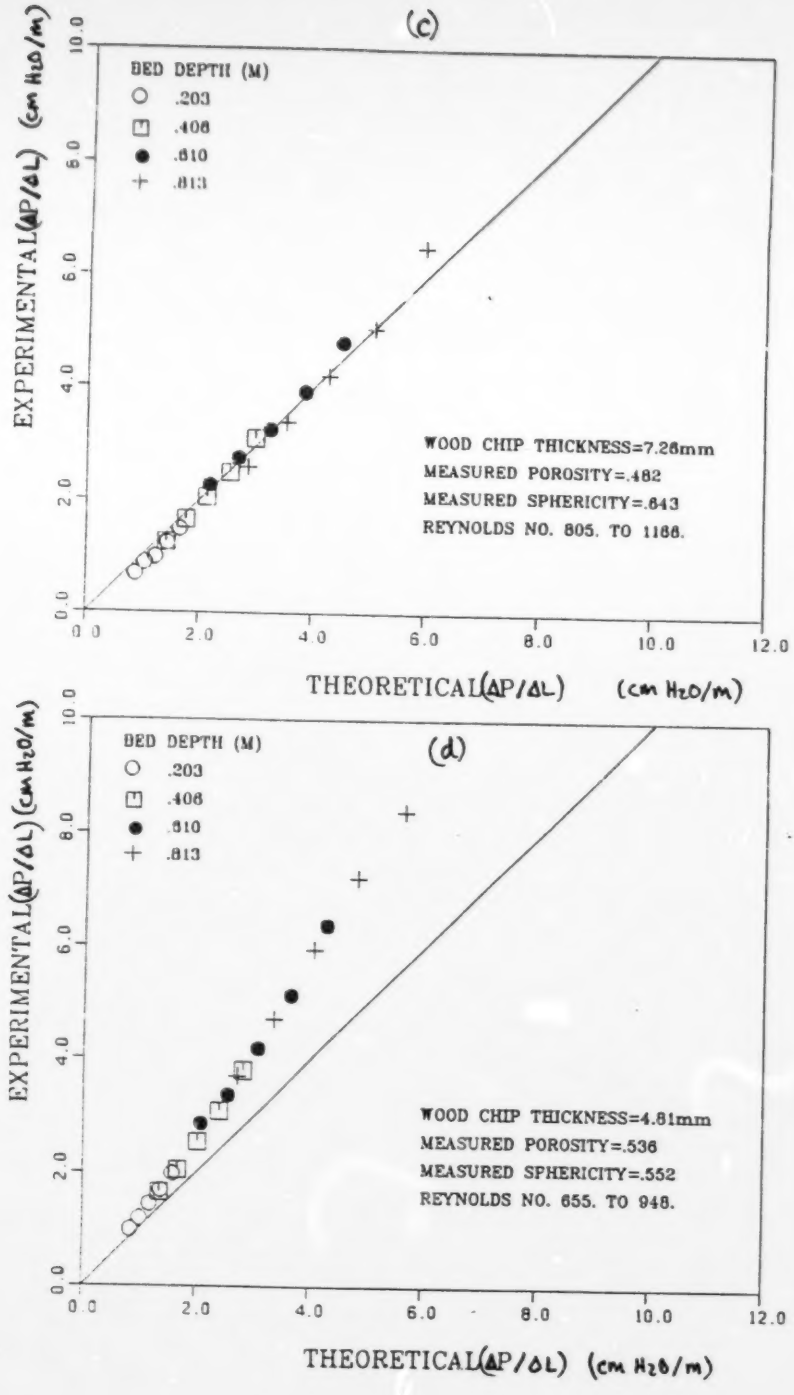

20. Experimental pressure drop versus Ergun equation prediction for wood chips of thickness
a) 2.44-mm b) 4.03-mm c) 7.26-mm d) 4.8 mm (mixed)

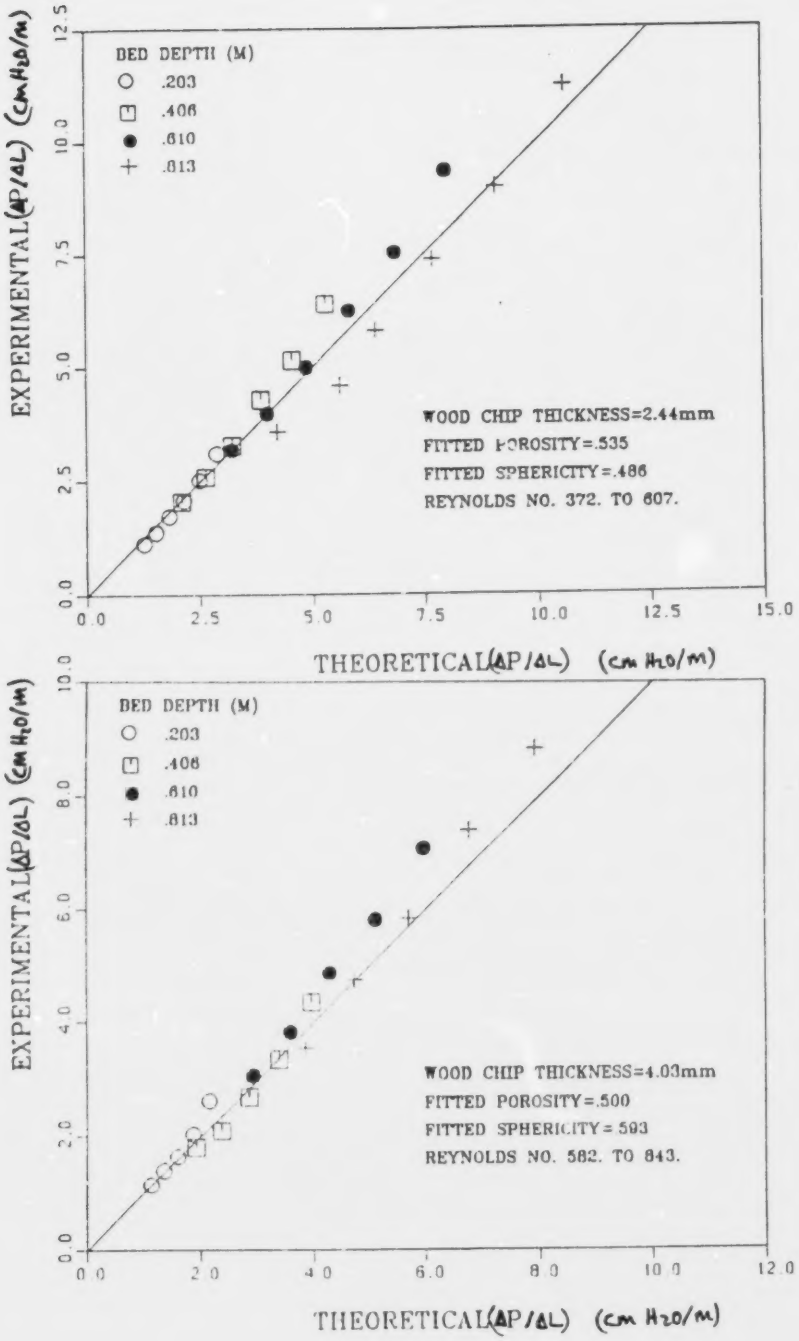

21. Experimental pressure drop versus Ergun equation predictions with fitted voidage and sphericity.

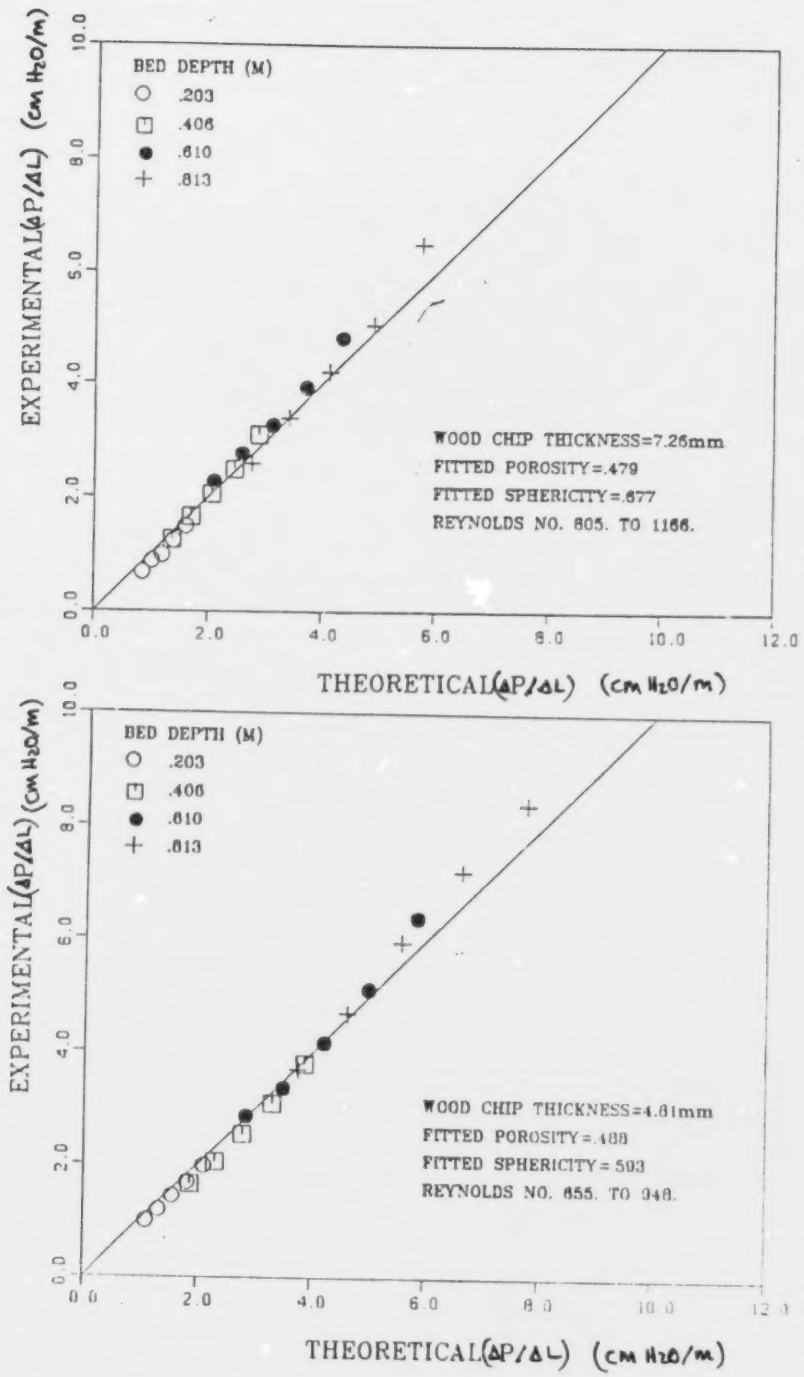

21. Experimental pressure drop versus Ergun equation predictions with fitted voidage and sphericity.

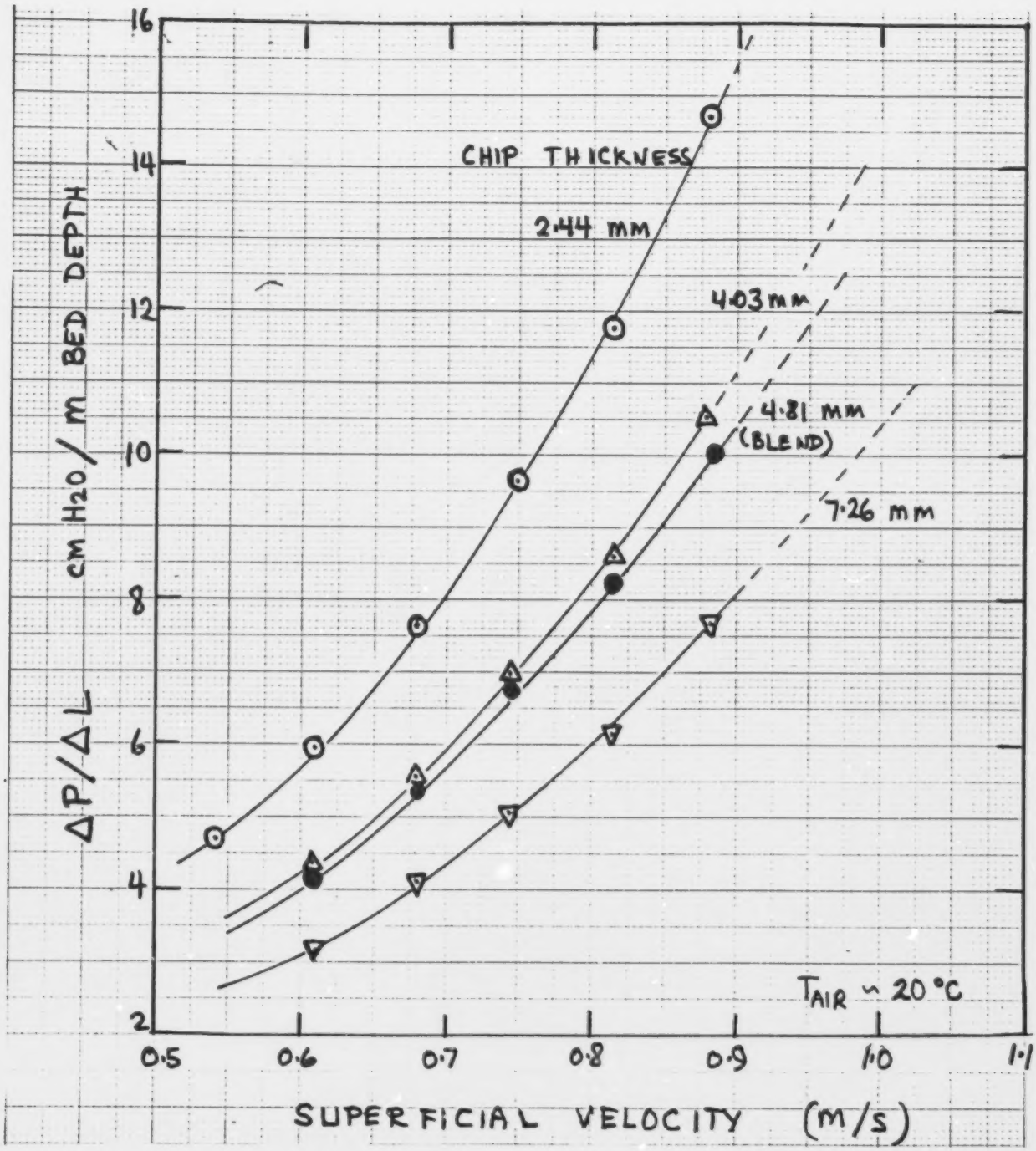

Fig. 22 Pressure Drop versus Velocity for Beds of Wood Chips

APPENDIX A Work Statement

Task No.	Description
1	Design silo, size and order other apparatus
2	Fabricate silo, pipe unit together, calibrate equipment
3	Pressure drop measurements on spherical particle to verify technique. Vary air velocity
4	Heat transfer measurements on spherical particles with dry air to verify technique. Vary air velocity and temperature. Compare with literature.
5	Heat transfer, pressure drop measurements on dry wood chips with dry air. Vary air velocity.
6	Heat transfer, pressure drop measurements on dry wood chips, with dry air. Vary chip size to check internal conduction effects.
7	Begin tests with moist chips and air. Vary inlet gas temperature and humidity.
8	Continue tests with moist chips. Vary chip size.
9	Continue tests with moist chips. Vary chip moisture.
10	Correlation of results. Mathematical modeling of process.
11	Final report and thesis.